SSRG International Journal of Civil Engineering
ISSN: 2348-8352/ https://doi.org/10.14445/23488352/IJCE-V11I8P105

Volume 11 Issue 8, 46-66, August 2024


*Original Article*

# Seismic Response Control of Tall Buildings Installed with Linear and Nonlinear Viscous Dampers

Bhargav S. Raval[1], Snehal V. Mevada[2]

[1]*Department of Civil Engineering, Gujarat Technological University, Ahmedabad, Gujarat, India.*
[2]*Department of Structural Engineering Department, Birla Vishvakarma Mahavidyalaya, Vallabh Vidyanagar, Gujarat, India.*

[1]*Corresponding Author : bhargavsraval@gmail.com*

Received: 06 June 2024 Revised: 14 July 2024 Accepted: 05 August 2024 Published: 29 August 2024

***Abstract*** *- With urbanization and world population growth, vertical development of cities is taking place, demanding the construction of safe and pleasant tall building structures. The safety of tall buildings under natural hazards is a critical area of study. Advanced vibration control techniques in engineering absorb and dissipate the forces of nature, ensuring stability and safety. Seismic vibration control strategies for a symmetrical 25-storey tall reinforced concrete building installed with passive linear and nonlinear viscous dampers are presented. The tall building is 3D modelled and designed using ETABS software. The dampers are installed at all storeys, and two further innovative alternate-storey damper arrangement schemes have been presented. With the damper arrangement schemes, the seismic responses of the system installed with passive linear and nonlinear viscous damper are obtained by numerically solving the equation of motion using the state space method in MATLAB under the considered earthquake time histories. For the linear and nonlinear viscous damper, the optimum damping coefficient(C) is determined. The controllability index is determined to study the effectiveness of linear and nonlinear viscous dampers. Top storey controlled peak responses are compared for the placement of damper with various arrangement schemes and corresponding uncontrolled peak responses; peak top storey displacement, top storey accelerations, storey drifts, storey displacement, storey acceleration, damper forces and effectiveness of each damper are evaluated. Alternate damper arrangement and nonlinear viscous damper are found to be quite effective in controlling the responses corresponding to uncontrolled responses.*

***Keywords*** *- Seismic response, Symmetric, Optimum, Passive linear viscous damper, Passive nonlinear viscous damper.*

## 1. Introduction

India's rapid population growth, urbanization, and rapid development have significantly increased the demand for vertical growth with pleasant, tall building structures that make efficient use of limited land resources while accommodating burgeoning urban populations. The stability of the tall structures against natural hazards, such as earthquakes and high winds, is paramount not only for the safety of their occupants but also for the resilience of urban infrastructure. In response to these challenges, structural engineering solutions have evolved to include active, semi-active, and passive systems designed to enhance the structural integrity and damping capacity of buildings. Among these, passive dampers have emerged as an important technology for their ability to dissipate seismic and wind energy without the need for external power, offering a reliable and maintenance-free solution to improve the performance of tall buildings. This attracts the researcher to investigate the seismic responses of tall building structures installed with passive linear and nonlinear viscous dampers. The motion of the structures produces relative motion within the damping devices, which is responsible for dissipating the energy. A discussion of the operation process and performance of passive energy dissipation systems has been studied (Constantinou and Symans,1992). The dynamic behavior of a fluid orifice damper examined steady-state cyclic load test data and a generalized mathematical model describing the linear as well as nonlinear behavior of a viscous damper (Symans and Constantinou,1998). The plan-wise characteristic parameter of supplement viscous damper and its distribution was identified to investigate the effectiveness of viscous damper on the reduction of edge deformation of asymmetric buildings and the effectiveness of viscous damper (Goel,1998). The basic principle and formulation of the mathematical model for SDOF, MDOF, energy-based design procedure and types of passive damper systems were presented (Soong and Dargush,1999). Fluid damper technology, consideration of analysis procedure, installation technique and its development for the protection of buildings, infrastructures like bridges and other types of structures are presented with destructive shock and vibration tests (Lee and Taylor,2001). The random forcing function used in wind tunnel test to perform nonlinear time history to predict the peak acceleration, the fundamental natural period of 5.26 seconds of a 39-storey office building installed with diagonal

and toggle brass passive energy dissipating fluid viscous dampers to reduce the wind generated acceleration response, cost-effectiveness was studied (Maknamara and Taylor, 2003). The dependency of viscous dampers on motion amplification device configuration, particularly for damper's stiffness. The complex modulus of viscous damper is used to represent a mathematical model with considered support brace's stiffness and damping values studied numerically for a 39-storey office building which was installed with toggle brace damper constructed on soft soil and a combined effect of the vertex shedding of an adjacent existing 52-storey building and earthquake effect to prove the effectiveness of damper (Huang, 2009). A 40-storey tower in New York City with the optimized structure to meet the strength requirement rather than adding mass and damping for TMD and suggesting the viscous dampers in tall buildings without increasing the weight of a building, and to allow the structure to be optimized for strength and acceleration separately was presented (Jackson and Scott, 2010).

The enhanced seismic performance objective was effectively achieved through the use of Nonlinear Viscous Damping Devices (NLVDD) with chevron brace, reverse toggle and scissor jack dampers combined with steel moment frames in a tall building structural system of the 12-storey San Bernardino Justice Center and 24-storey San Diego Central Courthouse building subjected to moderate and major earthquake ground shaking for the reduction in base shear demand, inter storey drift and acceleration (Sarikisian and Lee, 2013). A super tall residential building project which requires a higher human comfort level, located in Xiamen in southeast China, was studied to investigate the selection of viscous damping, optimal damper placement, and damper parameter optimization for the targeted additional damping ratio for wind-induced vibration comfort determined as 2% based on the wind tunnel test result and 1% for stiffness analysis. The investigation shows that large energy dissipation controls top-storey displacement with the application of viscous dampers (Ding and Zhao, 2016).

The backward difference formula was introduced to verify the equation of motion of wind-induced vibration for a 20-storey steel frame structure and compare it with conventional methods (Cheng, Zeng and Peng, 2017). The effectiveness of passive distributed vibration control viscous and viscoelastic devices arranged on multi-storey steel building frames was investigated during the life span of the building. The Newmark time marching scheme was adopted to solve the equation of motion of a multi-storey building. The response without and with the dampers was investigated to conclude the importance of damping ratio and modal frequencies to retrofit the building (Tathagata Roy and Vasant Matsagar, 2019). A brief review of vibration control of tall buildings installed with passive and active systems with their limitations, briefs about stochastic vibration control considering system parameters, and recent big data analysis are presented (Kavyashree and Patil, 2020). Chevron, diagonal and X-brass for seismically excited tall buildings installed with nonlinear fluid viscous damper studied with fast nonlinear analysis to evaluate the effectiveness of the damper system (Shariati and Kamgar, 2020). The performance of an Integrated Damping System (IDS) was studied by (Miguel and Ahmed, 2021). For the regular and irregular building configurations, damper placement issues were addressed as per the height of the building to optimize the dampers explored by (Huang and Bae, 2022). The buildings installed with the passive Tuned Mass Dampers (TMDs) and other passive damping offer significant benefits in reducing dynamic response in tall buildings, but they come with certain limitations. TMDs, for instance, are specifically tuned to a particular frequency, limiting their effectiveness to a narrow range of vibration and necessitating precise engineering to match the dynamic characteristic. Also, a large area with a large mass is to be attached at a high cost in the structural system installed with TMDs.

The friction and metallic yield dampers can introduce maintenance concerns due to wear and the potential need for replacement after a significant seismic event. These constraints highlight the versatility and reliability of viscous dampers, which operate effectively across a wide frequency range without the need for tuning and with minimal maintenance, making them a superior choice for enhancing the seismic resilience of tall buildings. However, comparatively less attention has been devoted to the nuanced potentials of linear and nonlinear viscous dampers in this domain, giving the opportunity for further exploration and innovation in utilizing viscous dampers to safeguard tall structures.

From the literature study, a noticeable gap has been identified in the damper installation strategies and optimum parameters for Linear Viscous Dampers (LVD) and nonlinear viscous dampers. Also, in light of the existing research, comprehensive investigation into Nonlinear Viscous Dampers (NLVD) is notably scarce for tall buildings.

This gap underlines the necessity of assessing the performance of LVD and NLVD across different arrangement schemes to get controlled response quantities of tall buildings. So, the aim of this research work is 1) To assess the effectiveness of three distinct damper arrangement schemes (I, II & III) and compare the performance of LVD and NLVD under each scheme, 2) To identify the most suitable damper arrangement scheme for LVD and NLVD damper in context of the considered tall building 3) To evaluate the effectiveness of damper in controlling various parameters like displacements, accelerations, storey drifts, storey displacements, storey accelerations. Present comparative analysis not only highlights the superior damper location schemes but contributes a novel perspective to the discourse on enhancing seismic resilience in tall systems through strategic damper optimization.

## 2. Structural Model

In the present study, the 25-storey tall reinforced cement concrete building is considered. The details are mentioned in Figure 1 and Table 1.

**Table 1. Properties and parameters for the considered tall building**

| Parameter | Value |
|---|---|
| Type of building | Special moment resisting frame. |
| Plan dimensions | 25m x 25m |
| No. of bays in X and Y directions | 5 |
| Bay width | 5m |
| Storey height | 3m |
| Size of beams | 300mm x 530mm |
| Size of columns | 750mm x 750mm |
| Thickness of the deck slab | 150mm. |
| Materials grades | Concrete: M35 – Slabs and beams, M50 – Columns.<br>Reinforcement Steel: $F_e$550<br>Masonry: Lightweight aerated cement block of 4.75 kN/m$^3$. |
| Codes | IS-875(I, II, III), IS-1893, IS-16700 |
| Loads | Floor finish load: 1 kN/m$^2$ at all types of floor level, 2 kN/m$^2$ at top floor level.<br>Live load: 3 kN/m$^2$ at all types of floor level, 1.5 kN/m$^2$ at top floor level. |

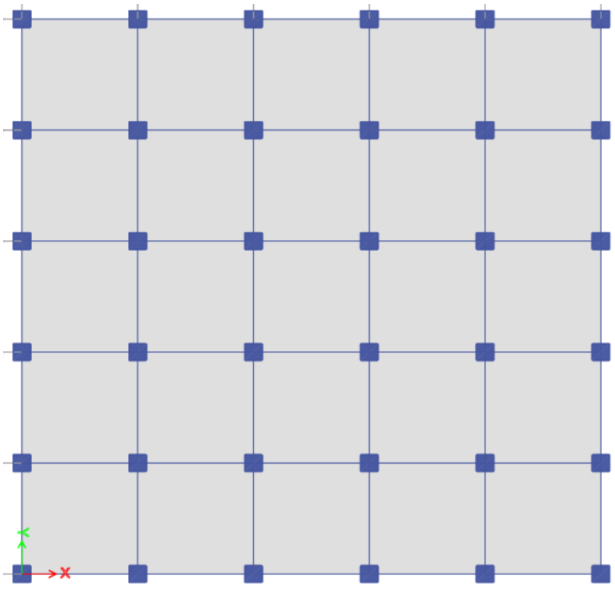

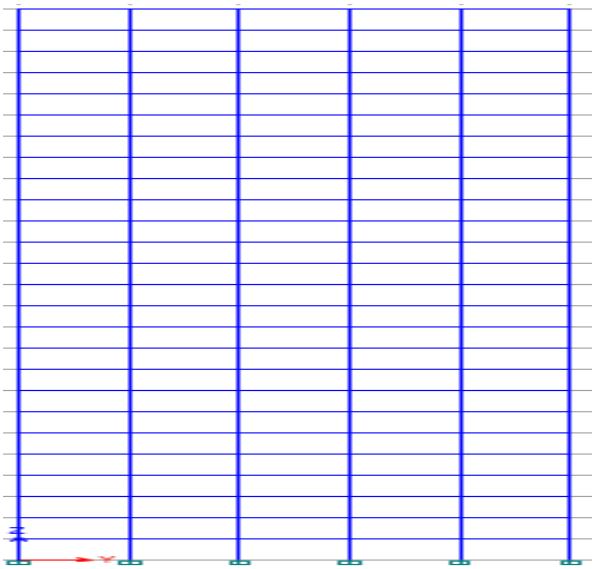

**Fig. 1 Plan and elevation of a 25-storey tall building**

The structural system under consideration is based on the following assumptions: 1) Rigid diaphragm is assumed 2) The superstructure is in linear range and obeys Hook's law. 3) The mass of the slab is uniformly distributed, so the Centre of Mass (CM) coincides with the geometrical centers of the floor slab. 4) Center of Mass (CM) and Center of Rigidity (CR) coincide. 5) The columns are axially rigid. The system is symmetrical about the X-axis.

The degree of freedom of structures considering static condensation is n-DOF is 25, one lateral translation $u_x$ of each floor in the X-direction.

## 3. Governing Equations of Motion

The governing equations of motion for a Multi Degree of Freedom (MDOF) system equipped with viscous dampers are as follows:

$$M\ddot{x}(t) + C\dot{x}(t) + Kx(t) = -M\Gamma\ddot{x}_g + \Lambda F \qquad (1)$$

For stories of n numbers, n represents the total degree of freedom, generally denoted as n-DOF, M denotes the mass matrix M, the damping matrix by C and the stiffness matrix by K, and they are symmetrical positive definite matrices of the system of size (n x n); $x = \{x_1, x_2, x_3 \ldots . x_n\}$T = the displacement vector of size (n x 1); $\dot{x}$(t) = Velocity of size (n x 1); $\ddot{x}$(t) = Acceleration of size (n x 1); $\ddot{x}$g = {$\ddot{x}$g , 0}T is ground excitation vector, $\ddot{x}$g is the ground acceleration in the x-direction. Γ denotes the influence coefficient vector of applied ground motion; Λ is the matrix that defines the location of the damper of size (n x n); F = {Fd1, Fd2, Fd3….Fdn}T is the vector of damper forces of size (2n x 1); Fd is the forces of the dampers along x-direction; F(t) = { $F_1$(t), $F_2$(t), $F_3$(t)….$F_n$(t)} is the vector of external force. The mass matrix is diagonalized as

$$[M] = \begin{bmatrix} m_1 & 0 & 0 \\ 0 & \ddots & 0 \\ 0 & 0 & m_{25} \end{bmatrix} \quad (2)$$

$$[K] = \begin{bmatrix} k_1 + k_2 & -k_2 & 0 & 0 & 0 \\ -k_2 & k_2 + k_3 & -k_3 & 0 & 0 \\ 0 & -k_3 & \ddots & 0 & 0 \\ 0 & 0 & 0 & k_{n-1} + k_n & -k_n \\ 0 & 0 & 0 & -k_n & k_n \end{bmatrix} \quad (3)$$

The damping matrix can be constructed from Rayleigh's damping. It offers a practical approach to approximating the damping behaviour in structural systems by utilizing the mass (M) proportional and stiffness (K) proportional matrices alongside the Rayleigh damping coefficients α and β.

In the present study, the damping effect of the structural system in dynamic analyses is calculated using Rayleigh's damping by considering 2% damping and considered for the first two modes of vibration. The Rayleigh's damping considers mass and stiffness proportional as,

$$C = \alpha M + \beta K \quad (4)$$

## 4. Computing Solution of Equations of Motion

The State Space Method is employed to solve the governing equations of motion (Hart & Wong, 2000; Lu, 2004).

The State Space Method analyses the response of the system using both displacements and velocities as independent variables. The equation is written as

$$\dot{Z} = A\ z + B\ F + E\ \ddot{x}_g \quad (5)$$

The two independent response variables are expressed as state vector z, where $z = [x \quad \dot{x}]T$. A is the system matrix of size (2n x 2n);

The distribution of control force is denoted by matrix B of size (2n x n), location matrix Λ of size (n x r), and E is the distribution matrix of excitations of size (2n x 1). These matrices can be written as:

$$A = \begin{bmatrix} 0 & I \\ -M^{-1}K & -M^{-1}C \end{bmatrix};\ B = \begin{bmatrix} 0 \\ -M^{-1}\ \Lambda \end{bmatrix} \quad (6)$$

and $E = -\begin{bmatrix} 0 \\ \Gamma \end{bmatrix}$

Where I is the identity matrix.

The solution can be written in an incremental form [Lu,2004] as

$$z[k+1] = A_d\ z[k] + B_d\ F[k] + E_d \ddot{x}_g \quad (7)$$

Where k denotes the time step; $A_d = e^{A\Delta t}$ of size (2n x 2n) is the matrix of the discrete-time system Δt as the time interval. The matrices containing the constant coefficient $B_d$ of size (2n x r) and $E_d$ (2n x 1) is written as:

$$B_d = A^{-1}(A_d - I)\ B \text{ and } E_d = = A^{-1}(A_d - I)\ E \quad (8)$$

Equation (8) is discretized in the time domain, and excitation force is assumed to be constant within any time interval. It can be written in a discrete-time form [Lu,2004].

## 5. Modelling of Fluid Viscous Damper

Fluid dampers work on the principle of fluid flow through orifices, generating forces that consistently resist structural movement during seismic and wind events. Figure 2 illustrates a schematic and mathematical model of the typical fluid viscous damper. A viscous damper consists of a body in a cylindrical shape with a central piston that moves through a fluid chamber. Silicon-based fluids are commonly used due to their ability to ensure reliable performance and stability. The force exerted by the damper is a result of differential pressure across the piston head (Symans and Constantinou, 1998; Lee and Taylor, 2001).

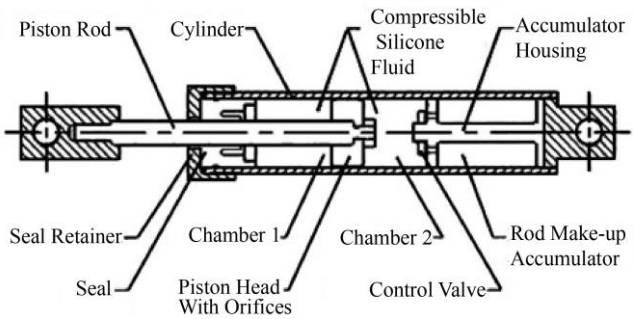


**(a) Schematic representation of Fluid viscous damper (Symans and Constantinou 1998)**

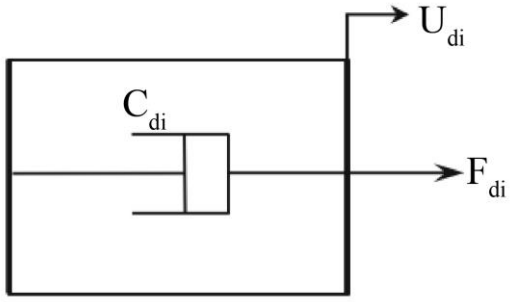


**(b) Mathematical representation of Fluid viscous damper**

**Fig. 2 Schematic & mathematical representation of the fluid viscous damper**

The output of a fluid viscous damper is a function of relative velocity between the damper ends as well as displacement and frequency. These devices are categorized into two types: linear viscous and nonlinear viscous.

The force $F_i$, in the viscous damper is proportional to the relative velocity between its ends and given by:

$$F_i = C_{di} |\dot{x_{di}}|^{\alpha} \text{sgn}(\dot{x_{di}}) \quad (9)$$

Where, $C_{di}$ is the damper coefficient of the $i^{th}$ damper, $\dot{x}_{di}$ is denoted by the relative velocity between the two ends of a damper. The relative velocity is considered to correspond to the position of the dampers. α is the damper exponent ranging from 0.2 to 1 for seismic applications (Soon and Dargush, 1997), and sgn(.) is the signum function. The orifices at the piston head primarily control the value of the exponent. When α = 1, a damper is called a Linear Viscous Damper (LVD) and with the value of α smaller than unity, a damper will behave as a Nonlinear Viscous Damper (NLVD). For seismic application, exponent α ranges between 0.1 and 1(Asher, 1996). Lower values of α dissipate a lot of energy in a short time. The dampers with α larger than unity have not been seen often in seismic practical applications, and the dampers with α more than unity (1.80 to 2) for wind application due to too much increase in temperature at the very low range of α for input wind lasting for days.

The greater the velocity, the greater the resisting force that is produced (Klembczyk, 2014) in fluid viscous dampers.

## 6. Numerical Study

Seismic response analysis for a 25-storey linearly symmetric tall reinforced cement concrete building installed with passive fluid linear and nonlinear viscous dampers is investigated by numerical simulation using MATLAB. The uncontrolled responses are derived by 3D analysis using ETABS software. A MATLAB program is prepared for uncontrolled and controlled responses.

The uncontrolled responses are compared between the software ETABS and the prepared MATLAB program. Uncontrolled responses were found to match the exact matches between ETABS software and the MATLAB program. Then, the controlled responses are derived using the MATLAB program under all real-time histories.

In this research, both linear and nonlinear viscous dampers are investigated. Damper arrangement schemes, scheme I, which entails the installation of dampers on each floor (Figure 3) with a total 25 numbers of dampers, and two innovative damper installation schemes II and III (Figure 3) entail the installation of dampers on alternate floors with 13 numbers of dampers and 12 numbers of dampers respectively. The analysis results of damper installation schemes for LVD and NLVD are compared in a numerical study. The key response quantities of interest include peak displacement and peak acceleration at the top storey, inter-storey drift, peak storey drift, peak storey displacement, peak storey acceleration and controllability index.

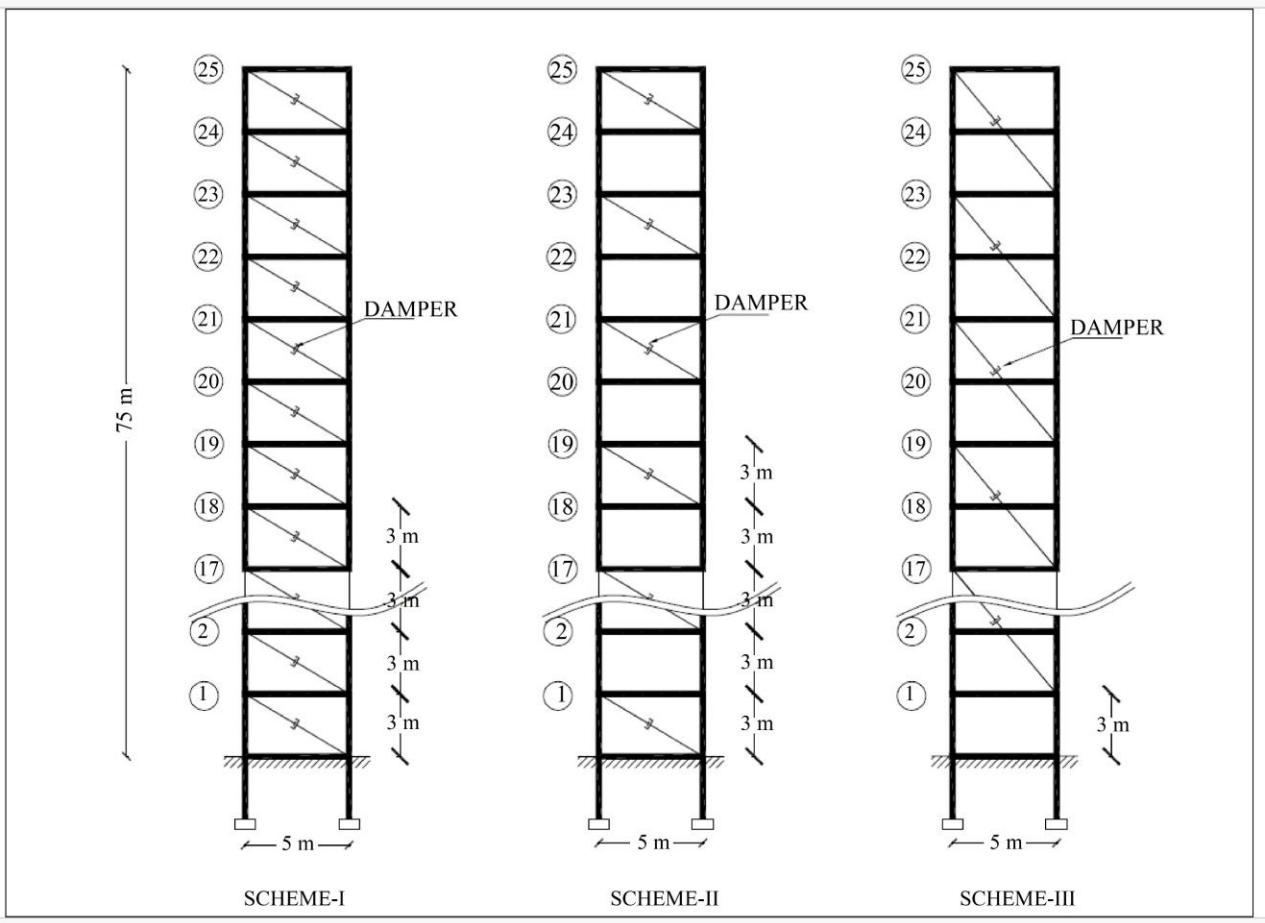


**Fig. 3 Damper arrangement schemes I, II & III. (I – All storey dampers, II & III – Alternate storey dampers)**

**Table 2. Details of earthquake motion used in the numerical study**

| Ground Motion | Recording Station | Component | Duration (sec) | PGA (g) |
|---|---|---|---|---|
| Imperial Valley, May 19th, 1994 | El Centro | LEC-180 | 40 | 0.31 |
| Loma Preita, October 18th, 1989 | Los Gatos Presentation Centre | LGP- 000 | 25 | 0.96 |
| North Ridge, January 17th, 1994 | Sylmar Converter Station | SCS-142 | 40 | 0.89 |
| Taiwan, September 20th, 1999 | Chi Chi | CHY-041-N | 90 | 0.64 |
| Southern California, June 28th,1992 | Landers | Cool Water | 28 | 0.42 |
| Bhuj, January 26th, 2001 | Ahmedabad | N | 80 | 1.03 |

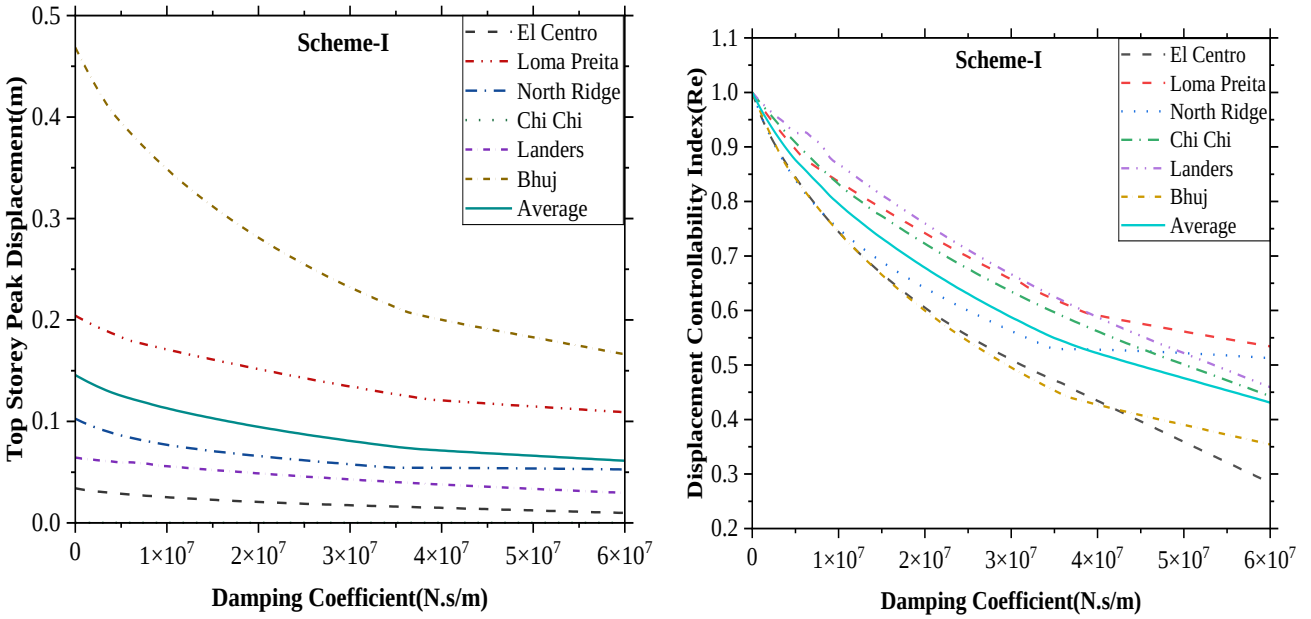


**Fig. 4 Top storey peak displacement responses and Controllability Index ($R_e$) for building installed with LVD and damper arrangement scheme-I under various earthquakes**

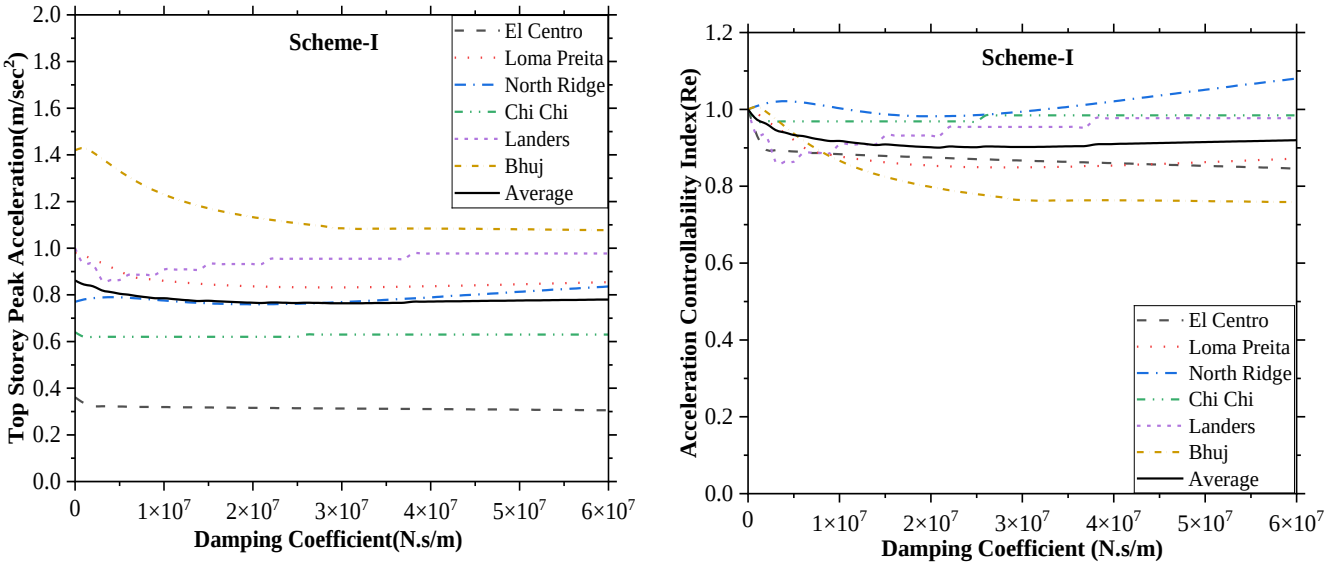


**Fig. 5 Top storey peak acceleration responses and Controllability Index ($R_e$)for the building installed with LVD and damper arrangement scheme-I under various earthquakes**

The responses are obtained for the key parameters mentioned above for six real earthquake ground motions: Imperial Valley (1940), Loma Preita (1989), Northridge (1994), Chi-Chi (1999), Landers (1929) and Bhuj (2001) with corresponding peak ground acceleration (PGA) values of 0.31g, 0.98g, 0.89g, 0.64g, 0.29g and 1.04g as detailed in Table 2.

### *6.1. Linear Viscous Damper (LVD)*

In order to study the effectiveness of proposed damper arrangement schemes with LVD and NLVD, the controllability index ($R_e$) is evaluated, which is a ratio of controlled to uncontrolled peak responses, offering a nuanced understanding of damper performance. Mathematically, $R_e$ can be written as follows:

$$R_e = \frac{\text{Peak response of controlled system}}{\text{Peak response of corresponding uncontrolled system}} \quad (10)$$

$R_e$ value less than one indicates that the implemented passive control system is effective in controlling the responses. $R_e$ value greater than one indicates that the response of a controlled symmetric tall system increases compared to an uncontrolled system. To determine the optimum value of the damping coefficient, the controllability index is determined and plotted (Figures 4 & 5) for the damping coefficient ranging from 1 x $10^6$ to 6 x $10^6$ N.s/m under considered earthquakes.

The damping coefficient(C) for various damper arrangement schemes (I, II, III) for LVD and NLVD dampers is optimized. The determined value of the optimum damping coefficient for LVD is 3 x $10^7$ N.s/m and 4 x $10^6$ N.s/m for NLVD (Figures 4 & 5).

The uncontrolled response of the considered tall system is compared with damper arrangement schemes I, II and III installed with LVD and NLVD. Peak displacement responses are considerably reduced in arrangement scheme-III as compared to arrangement scheme-II. The response is slightly reduced in scheme-I as compared to scheme-III. Similar behaviour is observed for acceleration response, storey drift, storey displacement, and storey acceleration.

The improvement of displacement responses is more compared to acceleration responses in scheme II and scheme III as compared to scheme I. With the help of the derived optimum value of the damping coefficient, the responses are plotted separately for damper each damper arrangement scheme–I, II and III under six considered earthquakes. Then, the numerical comparison is done (Figures 6 to 12).

As per Figures 6 & 8 with damper arrangement scheme-I, the observed top storey peak displacement response is reduced to 49%, 34%, 38%, 37%, 33%, 50% and an average of 40.16% considered earthquakes. Under the El Centro earthquake, controlled top-storey displacement is found to be 17.69mm as compared to uncontrolled 34.07mm. A similar trend is found in all considered earthquakes. With damper arrangement scheme II, top-storey displacement was reduced by 33%, 21%, 31%, 22%, 18% and 33% under six earthquakes. The average reduction is found to be 26.33%. With the damper arrangement scheme III, the reduction in top-storey displacement response is 48%, 33%, 43%, 35%, 19%, and 50%, an average of 38%. A slight difference in top-storey displacement response reduction in the system installed with scheme-I and scheme-III is observed. The average reduction in response is higher with scheme II than with schemes I and III.

From Figures 7 and 8, the top storey average peak acceleration response reduces to 31% in scheme I and 32% in schemes II and III. The peak top-storey acceleration is reduced from 20% to 35% by using schemes I and III. A similar response is observed in scheme I and III as compared to scheme II.

Figure 9 shows that the storey drift is highest from storey 1 to storey 7 and gradually decreases towards the top. The storey drift reduces up to 50% in most of the considered earthquakes with the use of scheme I & III as compared to scheme II.

From Figure 10, the percentage peak storey displacement response reducing with scheme-I 49%, 34%, 44%, 37%, 33% and 50%, respectively, for various considered earthquakes and the average reduction observed is 40.16%. With scheme II, 32%, 21%, 31%, 21%, 18%, 33% and average 26%. With scheme III, 48%, 33%, 43%, 36%, 19%, and 50%, the average reduction observed is 38.17%. This indicates that a similar response is found in scheme-I and scheme-III as compared to scheme-II. The performance of scheme-I and scheme-III are almost the same.

From Figure 11, the storey acceleration in the first five storeys is higher. Average storey acceleration response was reduced by 20% in scheme-I, 13.01% with scheme II, and less reduction by 5% in scheme III.

Figure 12 shows the hysteresis loops for the damper force as a function of displacement and velocity for the linear viscous damper. The hysteresis is plotted for scheme III, which shows results similar to those of arrangement scheme-I. The force-velocity loop indicates that the damper exhibits linear behavior as it is expected. The forces taken by the dampers are considerable.

This indicates tremendous seismic energy is absorbed by the dampers against all considered earthquakes, which in turn reduces the responses against seismic events. The larger the energy absorbed, the greater the response we derive from the installed dampers using the aforementioned damper installation schemes.

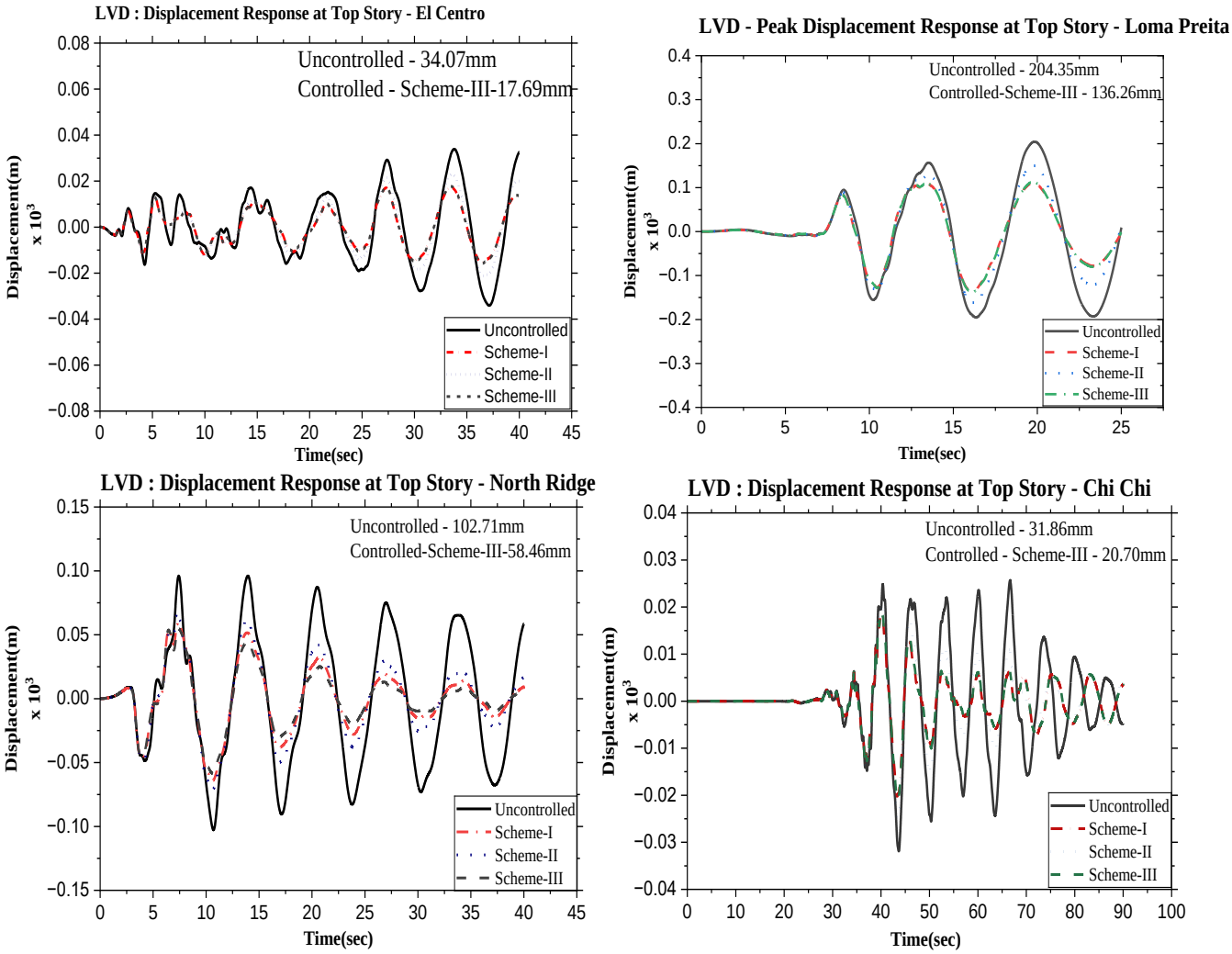


**Fig. 6 Comparison of top-storey displacement response with Scheme-I, II & III for the building installed with LVD under various earthquakes**

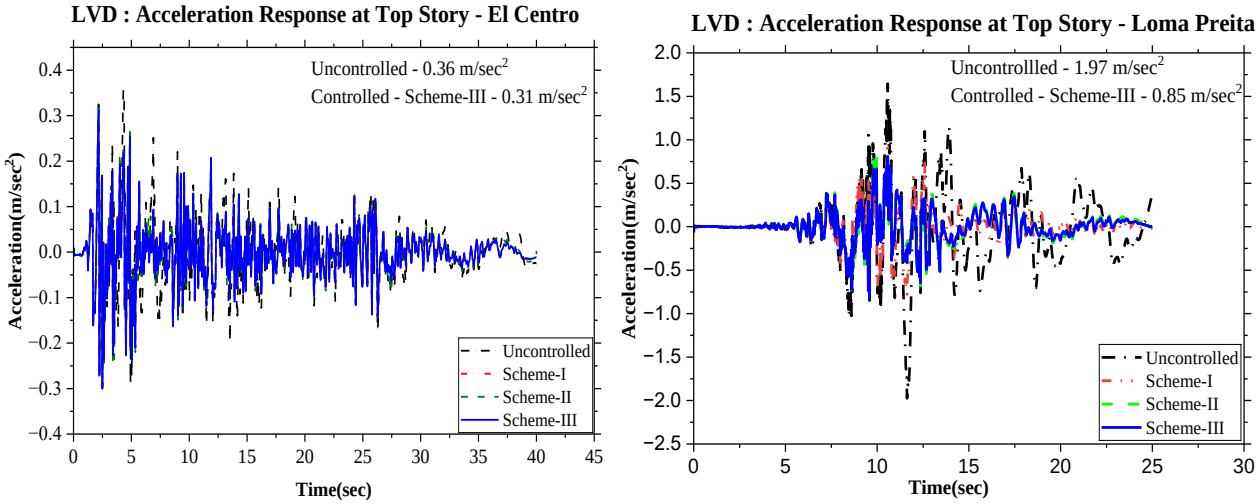


**Fig. 7 Comparison of top-storey acceleration response with Scheme-I, II & III for the building installed with LVD under various earthquakes**

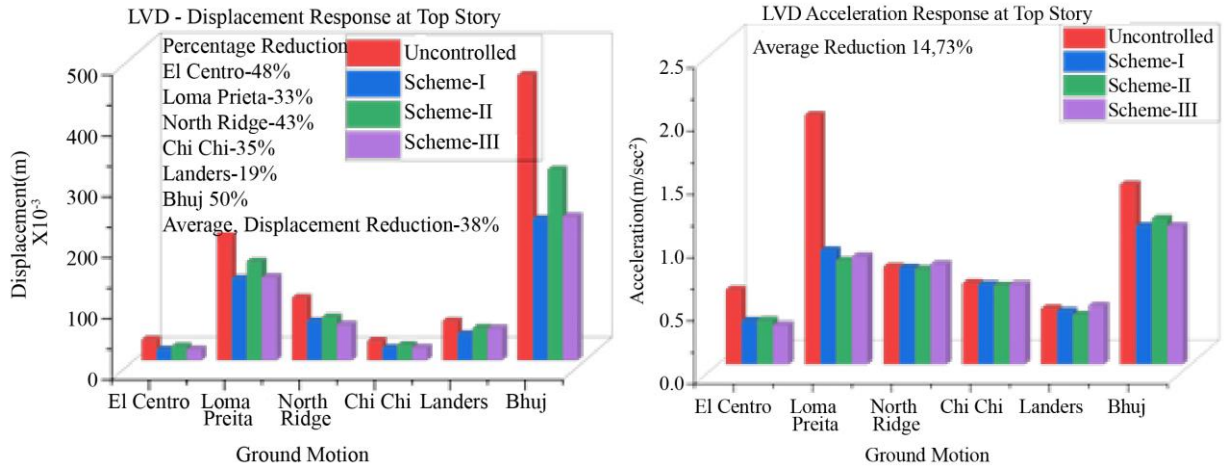


**Fig. 8 Comparison of percentage uncontrolled and controlled peak displacement and acceleration responses with scheme-I,II & III for the building installed with LVD**

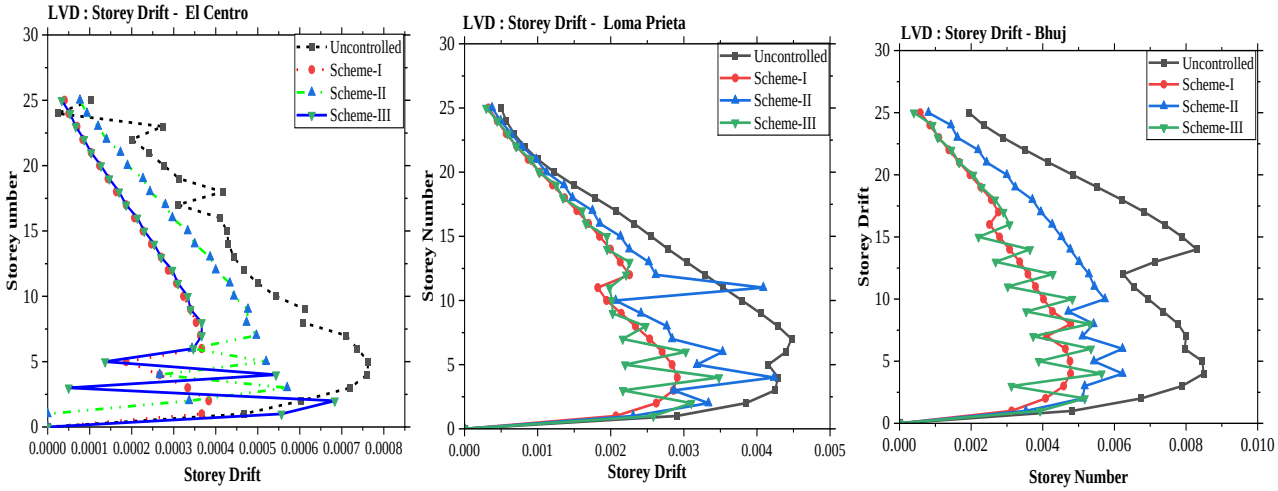


**Fig. 9 Comparison of uncontrolled and controlled storey drifts with scheme-I, II and III for the building installed with LVD under various earthquakes**

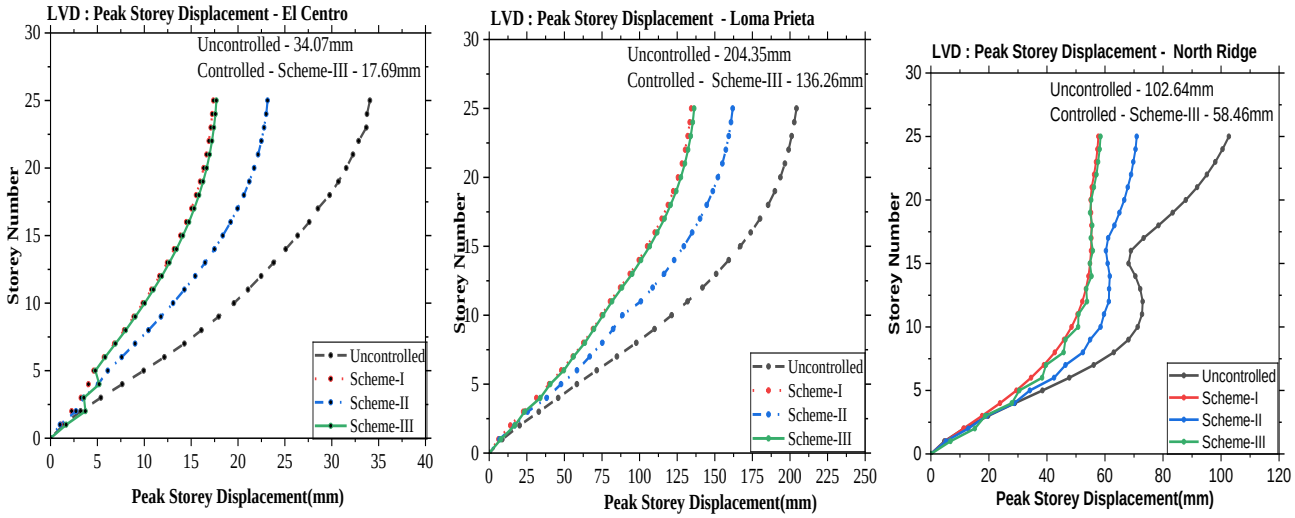


**Fig. 10 Comparison of uncontrolled and controlled storey displacement with Scheme-I, II and III for the building installed with LVD under various earthquakes**

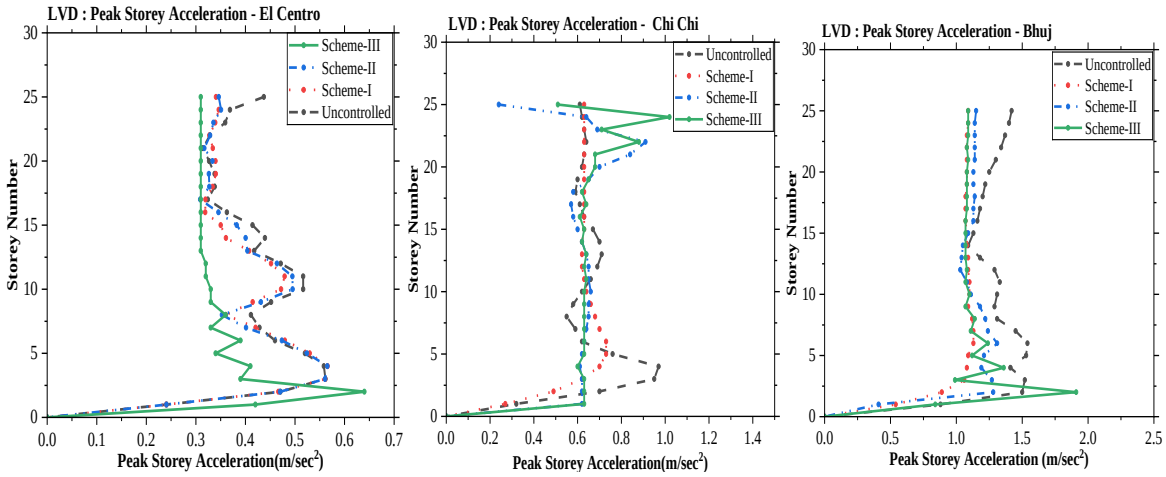


**Fig. 11 Comparison of uncontrolled and controlled peak storey acceleration with scheme-I, II and III under various earthquakes**

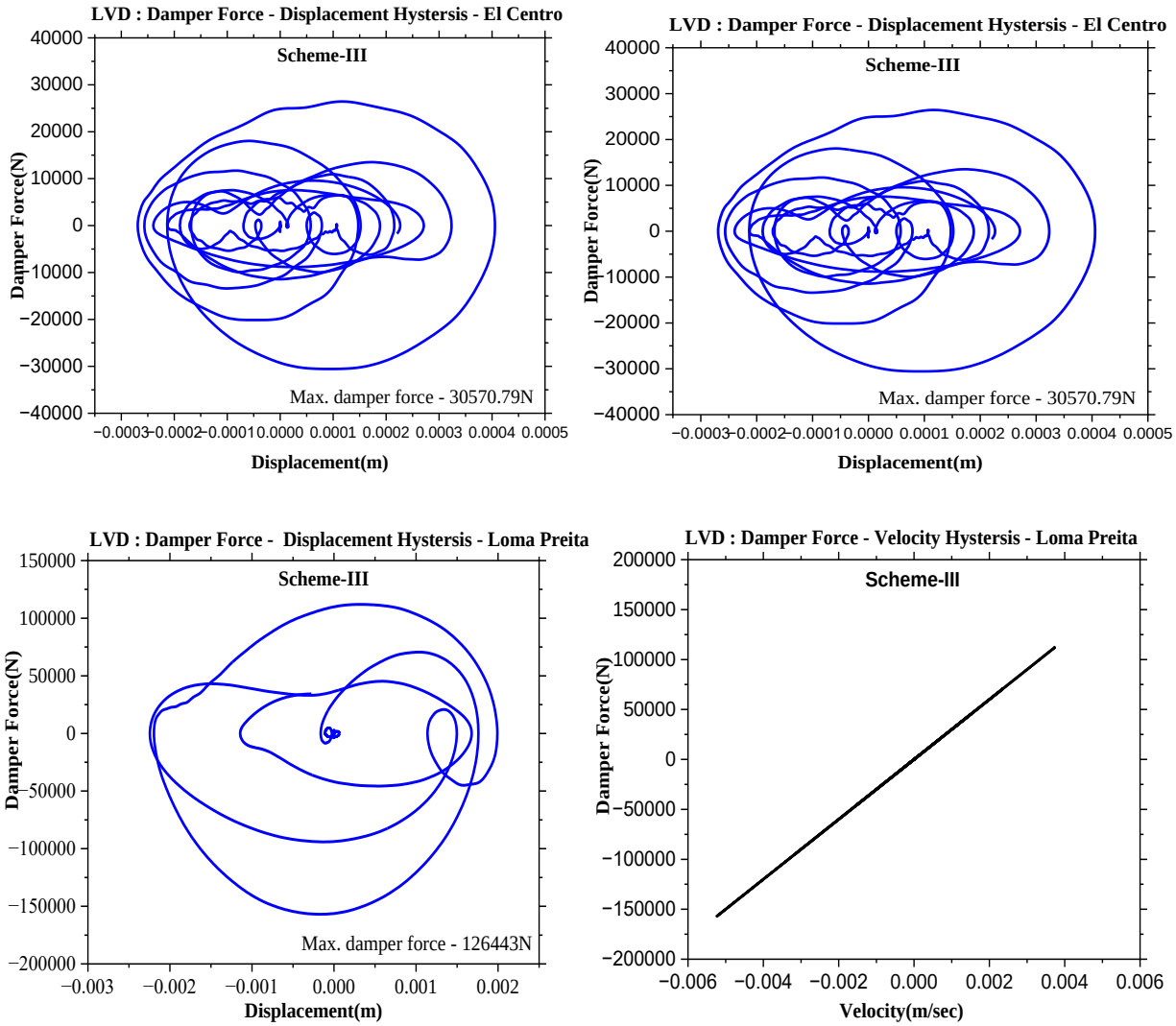


**Fig. 12 Typical hysteresis loops for LVD under El Centro (1994) and Loma Preita earthquakes (1989)**

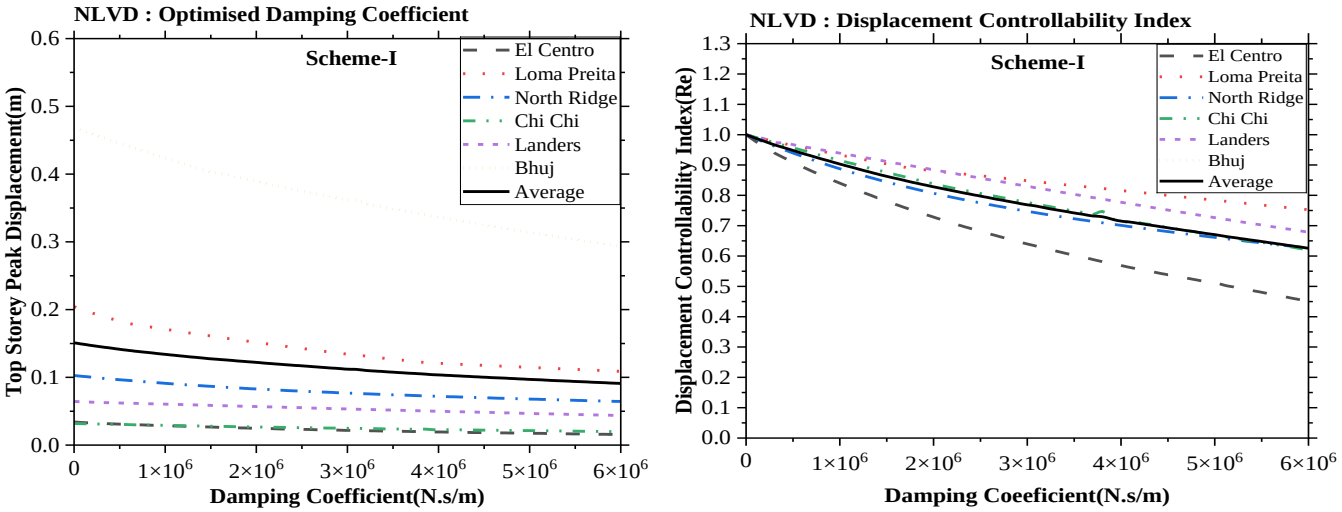


**Fig. 13 Top storey peak displacement responses and Controllability Index ($R_e$) for the building installed with NLVD under various earthquakes**

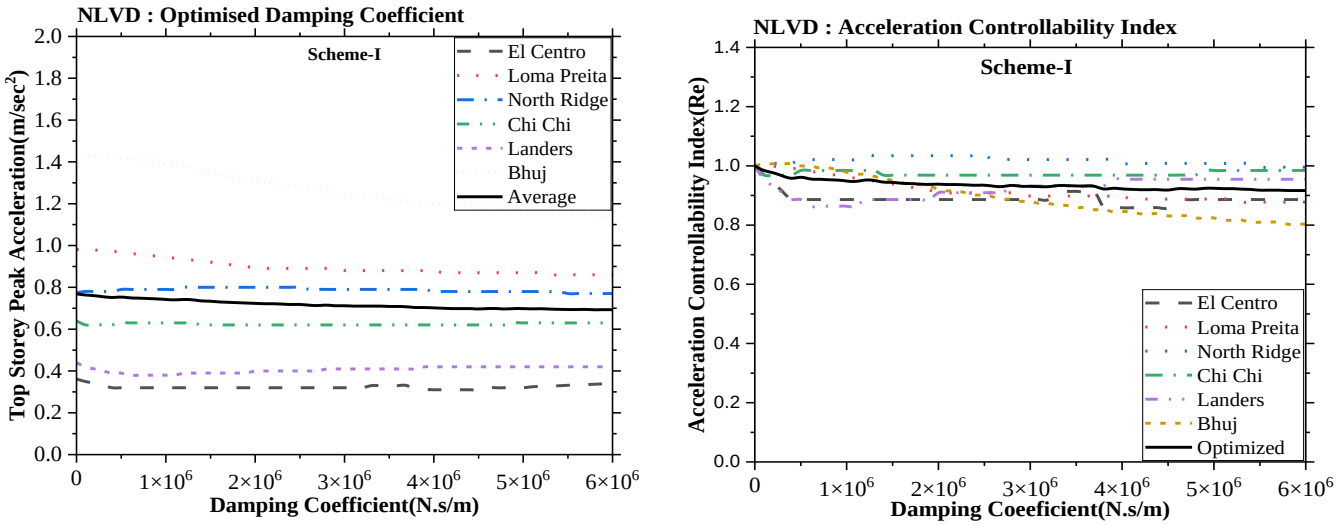


**Fig. 14 Top storey peak acceleration responses and Controllability Index ($R_e$) for the building installed with NLVD under various earthquakes**

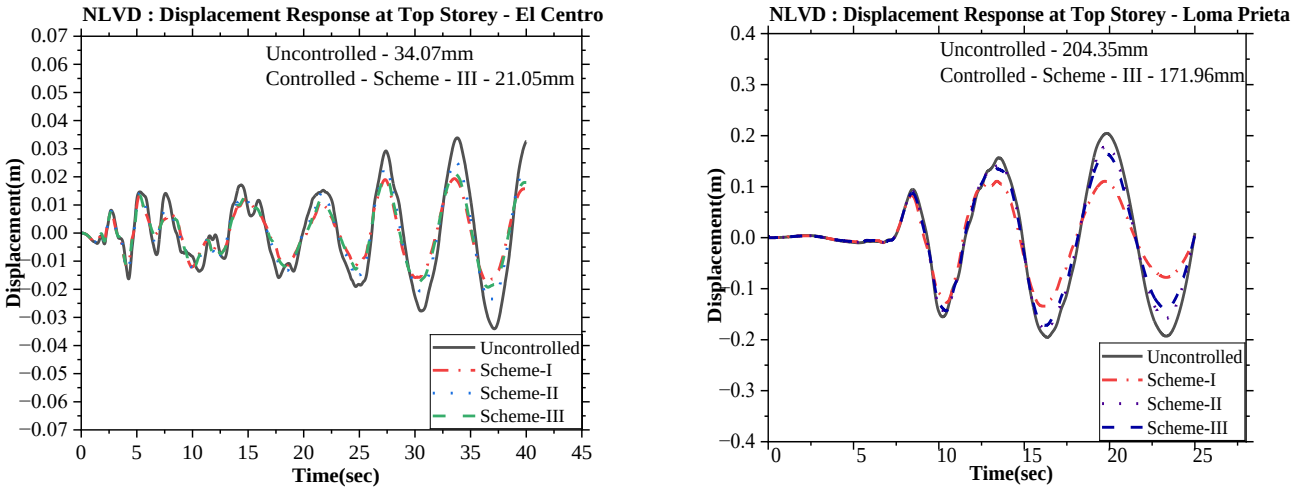

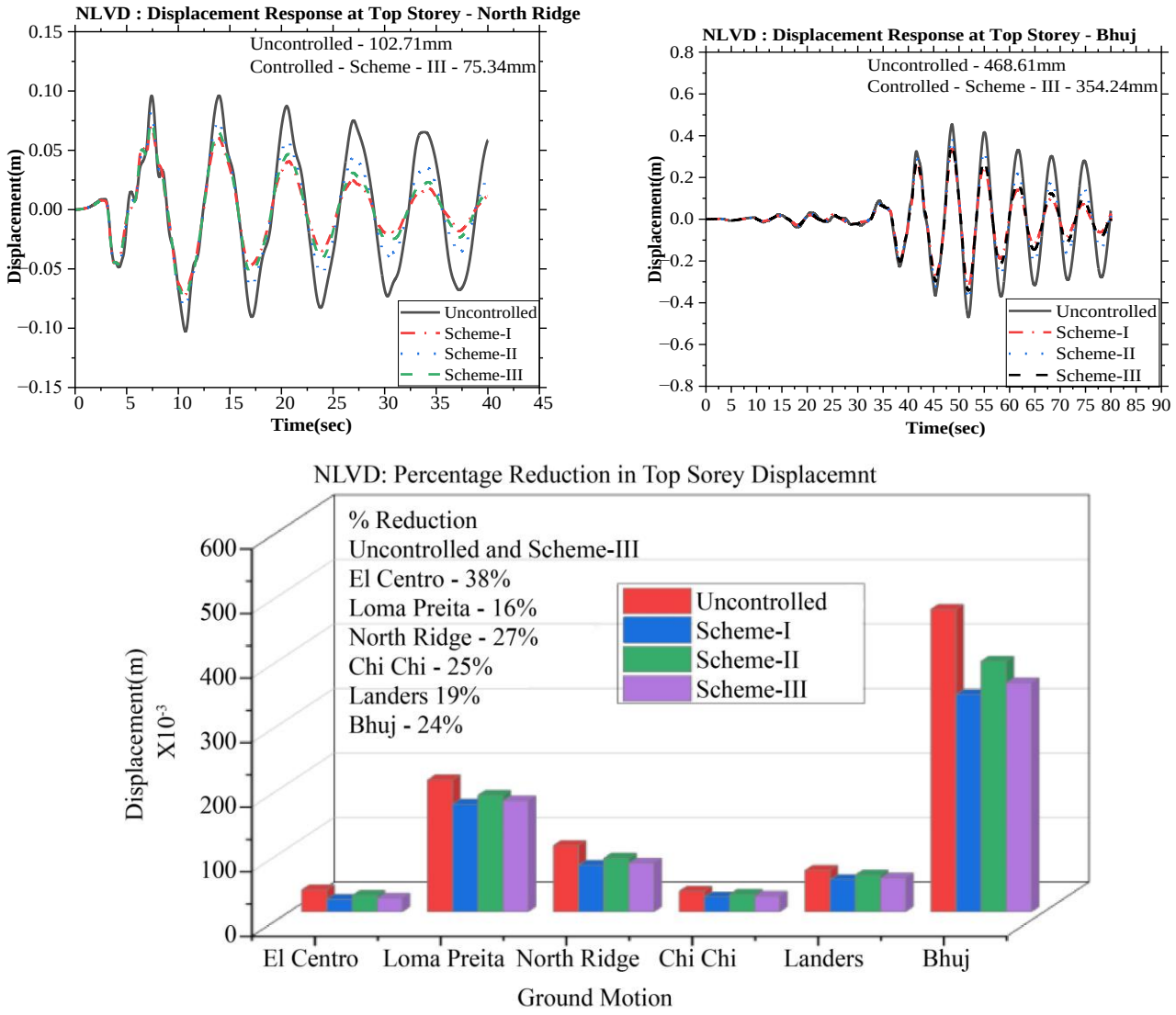


**Fig. 15 Top-storey displacement response and percentage-wise comparison with Scheme-I, II & III for the building installed with NLVD under various earthquakes**

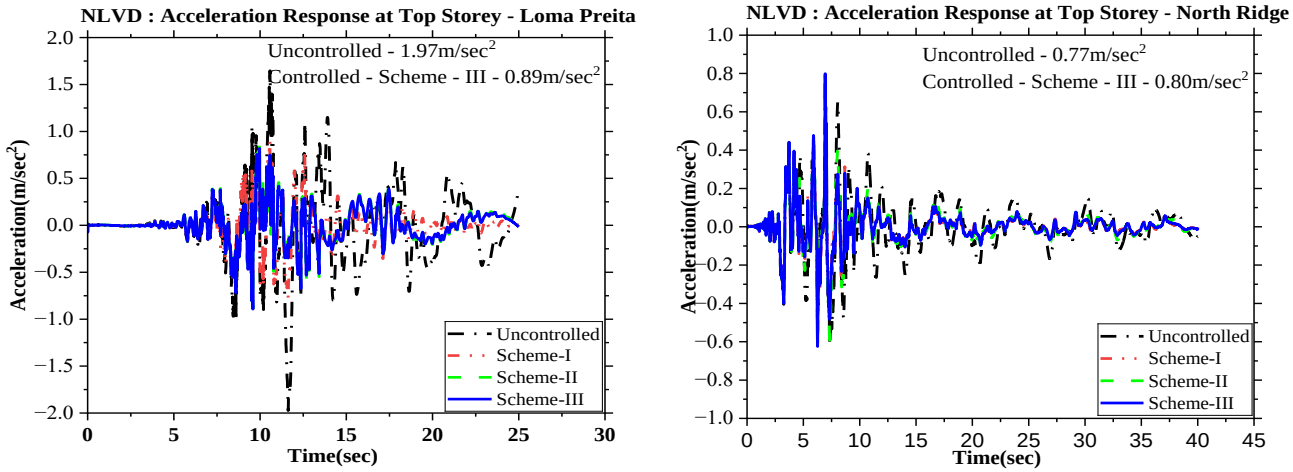


**Fig. 16 Comparison of top-storey acceleration response with Scheme-I, II & III for the building installed with NLVD under various earthquakes**

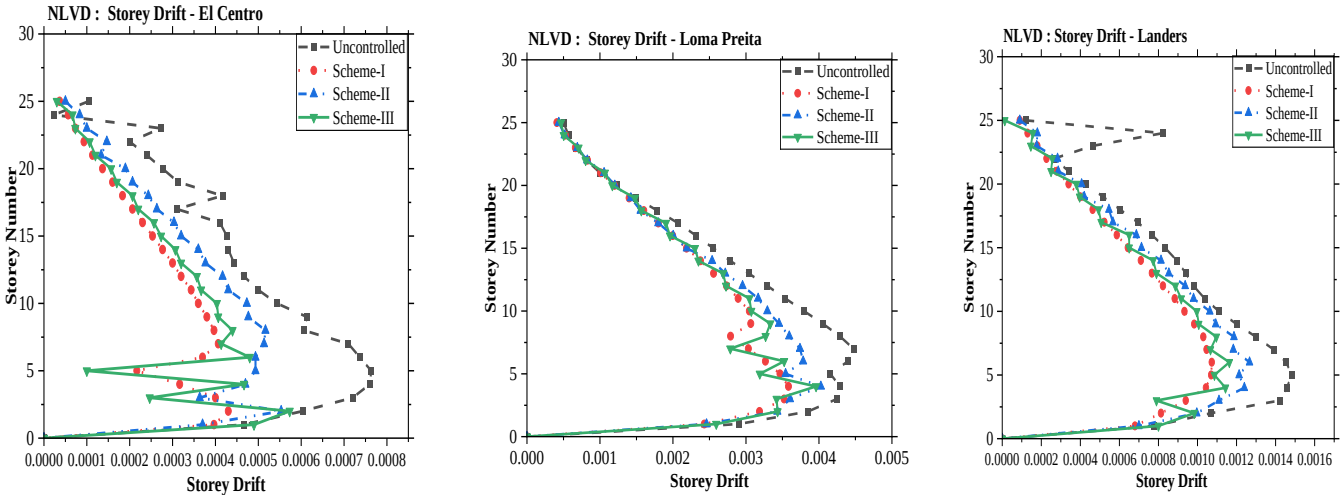


**Fig. 17 Comparison of uncontrolled and controlled storey drifts with scheme-I, II and III for the building installed with LVD under various earthquakes**

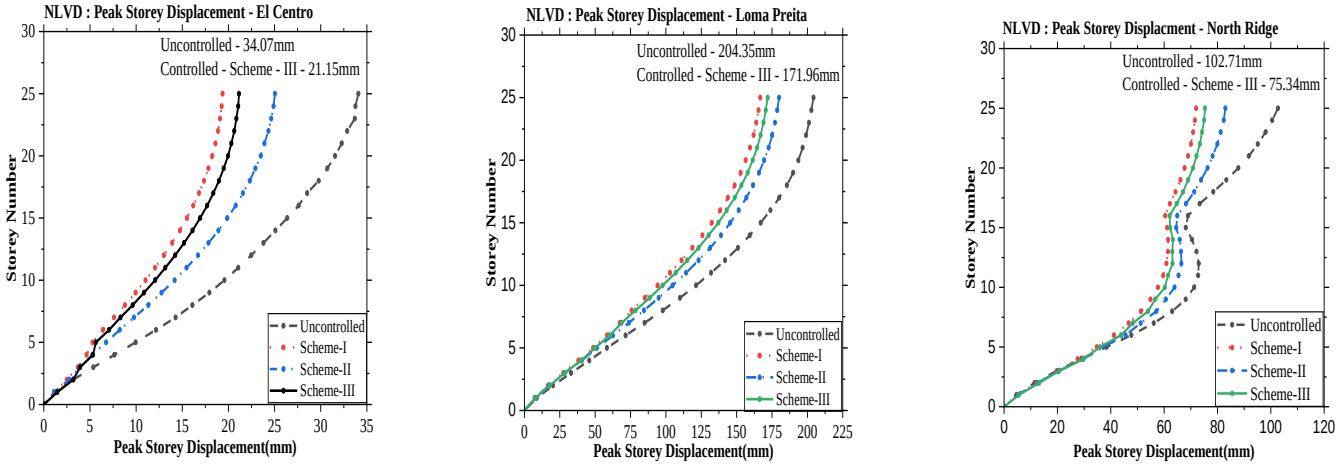


**Fig. 18 Comparison of uncontrolled and controlled storey displacement with scheme-I, II and III for the building installed with NLVD under various earthquakes**

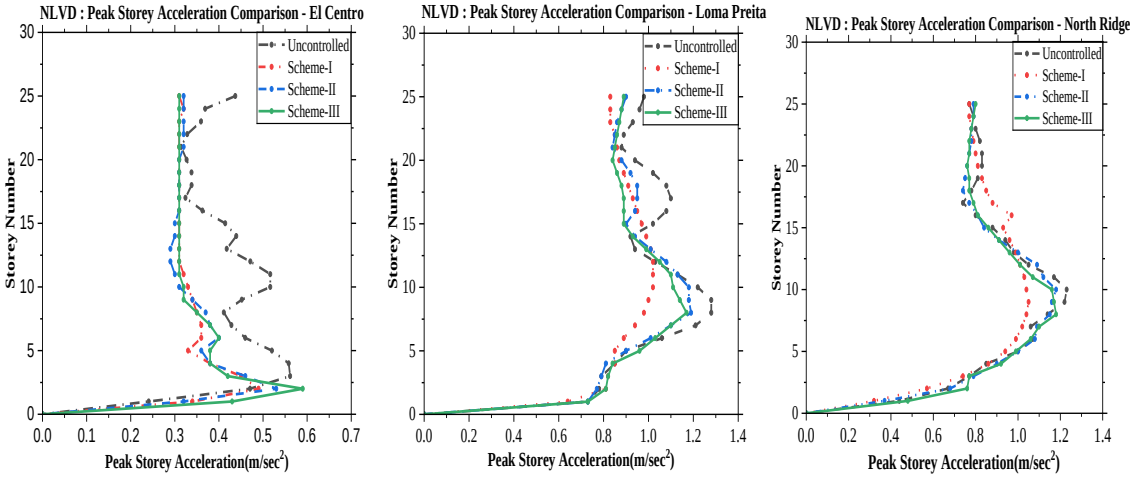


**Fig. 19 Comparison of uncontrolled and controlled storey acceleration with scheme-I,II and III for the building installed with NLVD under various earthquakes**

### *6.2. Nonlinear Viscous Damper (NLVD)*

This section focuses on the study of the nonlinear viscous damper. For the considered tall system, the distribution of mass and stiffness is uniform. The value of exponent α =0.75 is considered for study. Similar to LVD, the optimum damping coefficient is determined using the controllability index, 〖 R 〗_e. Figures 13 and 14 indicate that the optimum value of the damping coefficient is found to be 4 x 106 N.s/m. As per Figure 15, the top storey peak displacement responses reduced for considered earthquakes in percentage with scheme-I as 43%, 18%, 30%, 28%, 22%, 28% and average 8.16%. In scheme-II, 26%, 12%, 19%, 15%, 11%, 17% and average 16.67%, which is 11.49% more compared to scheme-I. Scheme-III 38%, 16%, 27%, 25%, 19%, 24% and average 24.83%. The value of top-storey displacement under the El Centro earthquake is 21.05mm as compared to the uncontrolled value of 34.07mm. Similar to the linear viscous damper, the numerical difference in top-storey displacement response with schemes I and III is 3% to 4%. Each plot displays both uncontrolled and controlled response numerical values for scheme III. From the trend of various plots and charts shown in Figure 15, the top-storey displacement response reduces by 19% to 38%.

Figure 16 shows that the top-storey acceleration responses reduce with scheme-I by a maximum of 45%. Compared to the uncontrolled top-storey acceleration response of 1.97m/sec$^2$, the controlled response is 0.89 m/sec$^2$ with scheme-III under the Loma Preita earthquake. A similar trend is observed for considered earthquakes, except acceleration response increases under the North Ridge earthquake by 3% due to the nature of the earthquake. With scheme II, the top storey acceleration response reduces by 11%, 54%, 1.31%, 3%, 11%, 8% and an average of 14.72%. Now, with scheme III, the response reduces to 14%, 55%, 1.35%, 3%, 7%, 12%, and an average of 15.39%. The results show that using schemes I, II and III, the observed response reduction is almost the same, with less than 1% difference between schemes I and III. For the North Ridge, Chi Chi and Landers earthquakes, the top-storey displacement response reduces more than the acceleration response. Figure 17, similar to the LVD, uses NLVD, and the storey drift is more in storey-1 to storey-10. The reduction in storey drift was observed as a maximum of 44% in scheme-I, 28% with scheme II and 45% in scheme III. The result shows that the damper performance to reduce the storey drift is almost the same in the scheme I and III as compared to scheme II. Figure 18 is similar to LVD; the storey peak displacement is higher from storey-15 to storey-25. The peak storey displacement response compared to the uncontrolled system is reduced to 43%, 18%, 30%, 28%, 22%, 28%, and the average reduction found is 28.17% with scheme-I, 12.33% with scheme-II, and 38%, 16%, 27%, 25%, 19%, 24% and average reduction found is 24.83%. The observed difference in controlled response reduction in schemes I and III is only 3.34%. Figure 19, Peak storey acceleration reduces with a maximum of 23% with scheme-I, 7.17% with scheme-II and 4.98%. Peak storey acceleration increases at storey-2 under El Centro and Bhuj earthquake with scheme III, but in all remaining storeys, it reduces. Higher peak storey acceleration at storey-1 to storey-5 and storey-15 to storey-20. Scheme I reduces higher acceleration compared to scheme III. Figure 20 shows the hysteresis loops for the damper force as a function of displacement and velocity for the nonlinear viscous damper. The force-velocity loop reveals that the damper exhibits nonlinear behavior. The higher the velocity, the more considerable force is taken by the damper showing the effectiveness of the damper. Here, the forces taken by the dampers with scheme III are greater than those taken by LVD with the use of the same scheme.

The study shows that the various response quantities derived using nonlinear viscous dampers using the considered damper arrangement schemes I, II and III are quite comparable. The top-storey displacement response and top-storey acceleration response were reduced considerably. The optimum damper coefficient required is also small compared to linear viscous dampers. Also, the storey drifts, storey displacement, and storey acceleration responses are similarly reduced. This needs to study the comparison between linear and nonlinear viscous dampers.

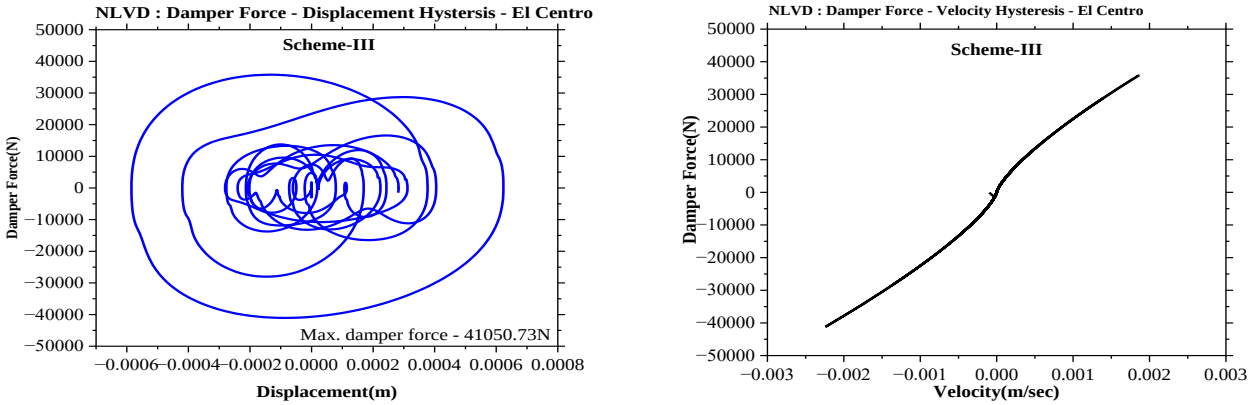


**Fig. 20 Typical hysteresis loops for NLVD with scheme-III under El Centro (1994)**

### *6.3. Comparison between Linear and Nonlinear Viscous Damper*

**Table 3. Comparison of various damper installation schemes for LVD & NLVD**

| Ground Motion | Uncontrolled Displacement (mm) | Controlled Top Storey Displacement Response (mm) | | | | | |
|---|---|---|---|---|---|---|---|
| | | Scheme-I | | Scheme-II | | Scheme-III | |
| | | LVD | NLVD | LVD | NLVD | LVD | NLVD |
| El Centro | 34.07 | 17.37 | 19.37 | 23.16 | 25.32 | 17.69 | 21.15 |
| Loma Preita | 204.35 | 134.35 | 166.74 | 161.93 | 180.47 | 136.26 | 171.96 |
| North Ridge | 102.71 | 64.11 | 72.00 | 70.95 | 82.98 | 58.46 | 75.34 |
| Chi Chi | 31.86 | 20.22 | 22.96 | 25.04 | 26.93 | 20.70 | 24.04 |
| Landers | 64.10 | 42.86 | 49.98 | 52.71 | 56.98 | 52.07 | 52.30 |
| Bhuj | 468.61 | 232.17 | 336.59 | 313.04 | 388.25 | 236.49 | 354.54 |

In this section, a comparison of tall buildings considered to be installed with LVD and NLVD is made. Responses of a tall system with a damper arrangement scheme (I, II & III) have been studied in sections 6.1 & 6.2 with derived optimum damping coefficient. The damper arrangement schemes I and III are quite comparable. Further study is required to identify the most effective damper out of LVD and NLVD. The study further extends to compare linear and nonlinear viscous dampers to determine the most suitable damper type and optimal damper arrangement scheme-I & III. By comparing LVD and NLVD installed with damper arrangement scheme-I, the controlled top-storey peak displacement response reduces by 49%, 38%, and 33%, as per Figure 21 and Table 3. Also, with the LVD, the average top-storey peak displacement response reduces to 40.16%. NLVD and scheme I reduce the response to 43%, 31%, 28%. The observed difference in top-storey displacement response, expressed as a percentage, decreases by 10 – 11% for the tall system installed with LVD and NLVD.

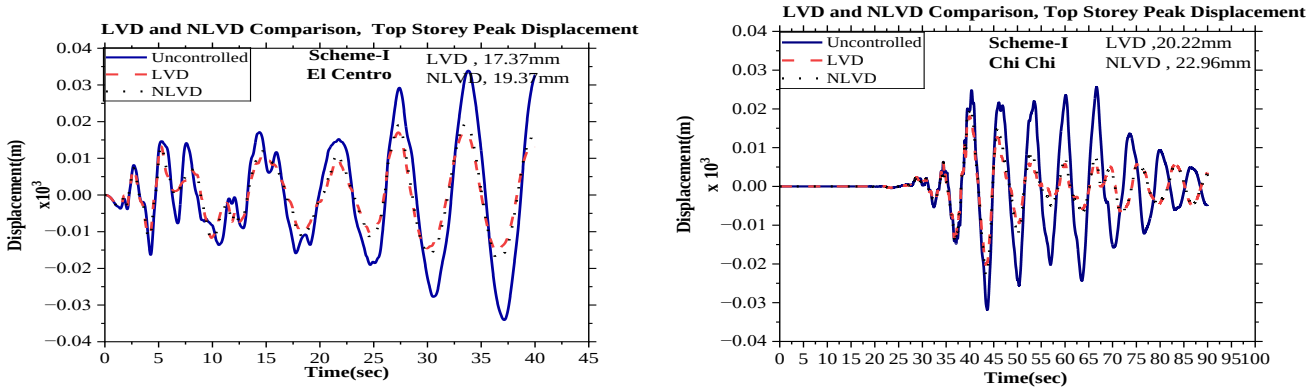


**Fig. 21 Comparison of top-storey peak displacement for LVD and NLVD installed with scheme-I under El Centro and Chi Chi earthquake.**

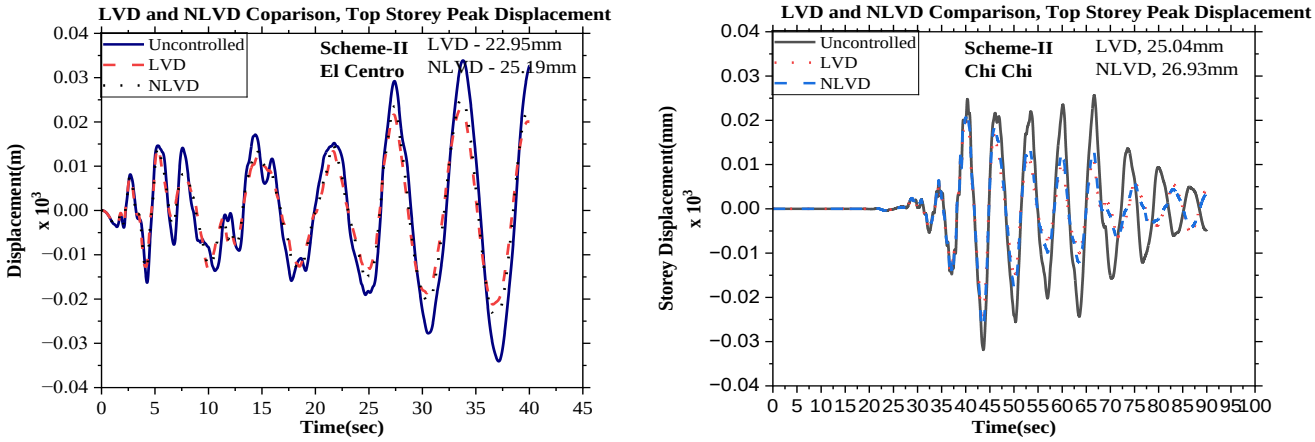


**Fig. 22 Comparison of top-storey peak displacement for LVD and NLVD installed with scheme-II under El Centro and Chi Chi earthquake.**

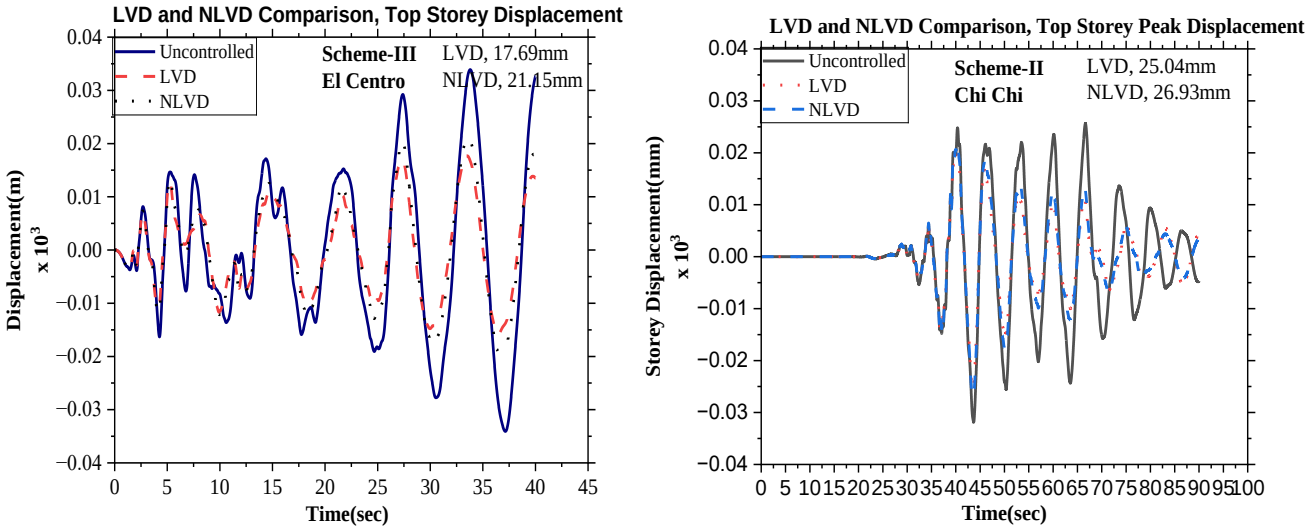


**Fig. 23 Comparison of top-storey peak displacement for LVD and NLVD installed with scheme-III under El Centro and Chi Chi earthquake**

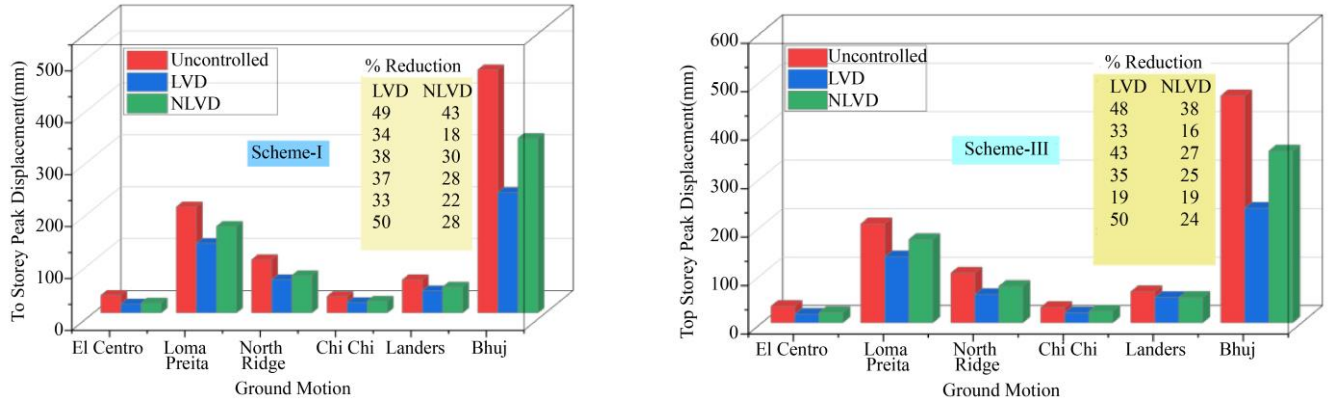


**Fig. 24 Percentage reduction in top storey peak displacement with scheme-I & III for the tall building installed with LVD & NLVD**

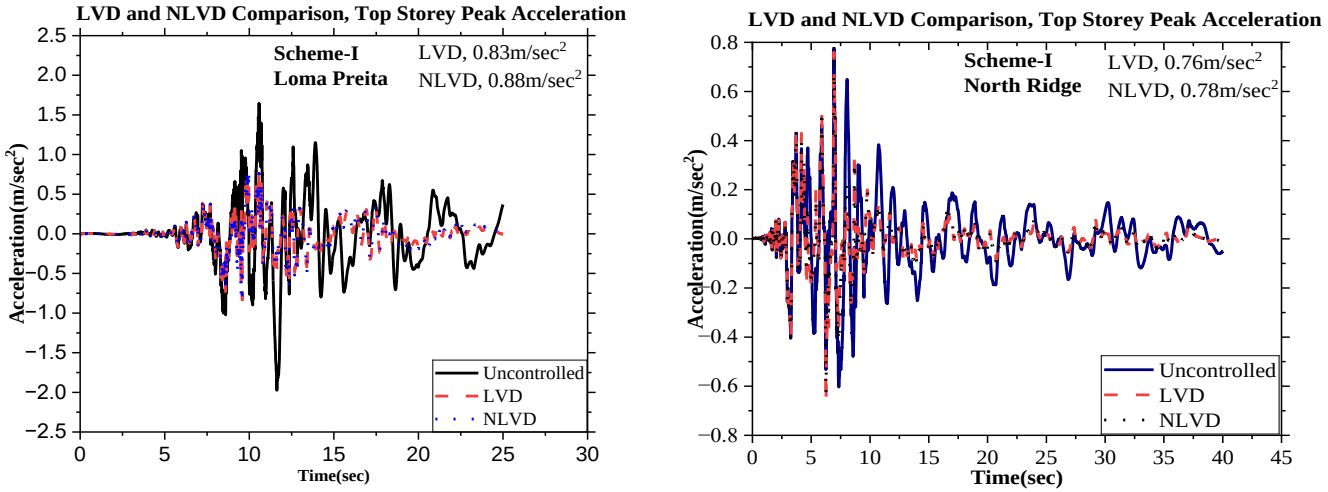

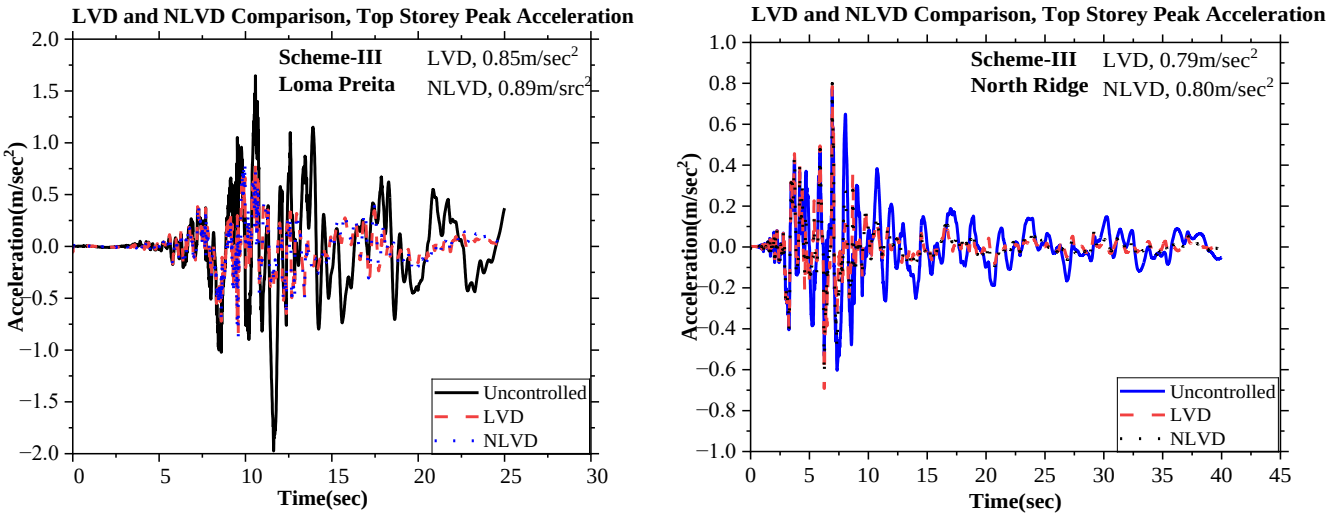


**Fig. 25 Comparison of LVD and NLVD top storey acceleration response with scheme-I & III under Loma Preita and North Ridge earthquake**

Figure 25 shows that with scheme-I, the top storey acceleration response reduces from 14% to 58% for the tall system installed with LVD and a similar reduction is observed for NLVD. Under the Loma Prieta earthquake, the observed top-storey acceleration is 0.83 m/sec$^2$ for the LVD and 0.88 m/sec$^2$ for the NLVD with scheme-I. Slightly higher values in top storey acceleration response were found with scheme-III as 0.85 m/sec$^2$ for LVD and 0.89 m/sec$^2$. The difference in top-storey acceleration between schemes I and III is 1% to 3%. It is also observed that acceleration reduction is less in the case of NLVD than in LVD due to the exponent effect. From Figures 9 and 17, it is observed that the scheme-II arrangement of dampers is found to be less effective than schemes I and III. For storey drift response, the results observed for LVD schemes I and III show the maximum reduction in drift is up to 56% with type LVD and 50% with type NLVD. A similar observation is found for scheme III. The LVD shows more drift control than NLVD, and scheme-I gives better controllability than scheme-III. Figure 27 shows a comparison of storey peak displacement response for schemes I and III. It is observed that both the schemes are comparable, with only slight variations in response for type LVD and NLVD. Scheme-I and scheme-III have a storey displacement reduction difference of 10-15%. The maximum storey displacement reduction for LVD with scheme-I is 49%, and with scheme III, it is observed at 48%. For the NLVD with scheme-I, 43% with scheme-I and 38% with scheme-III observed. Similar responses are found for all six earthquakes.

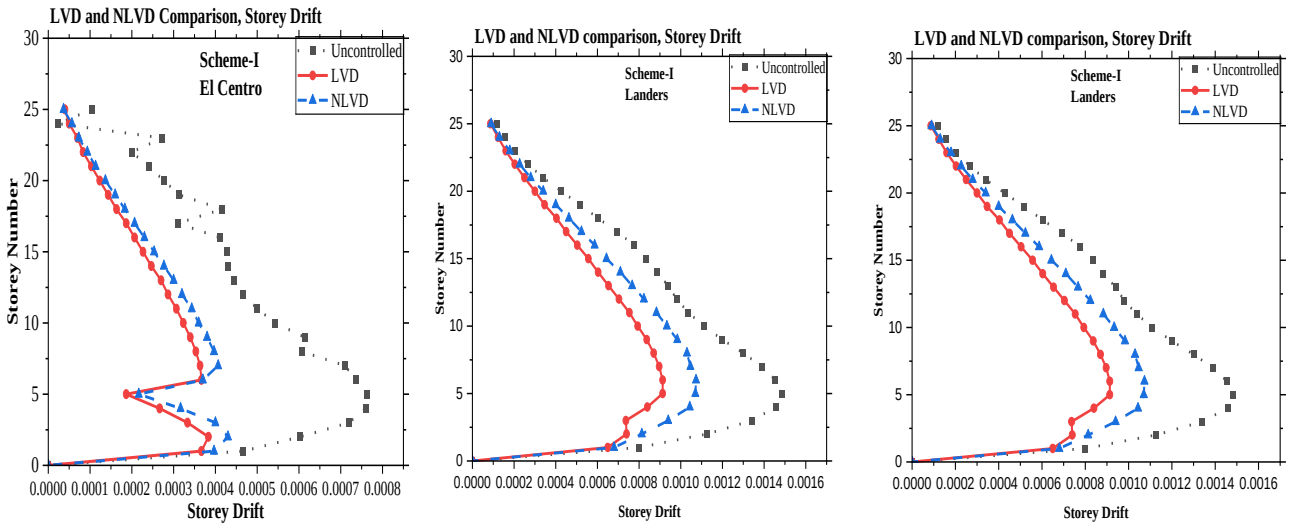

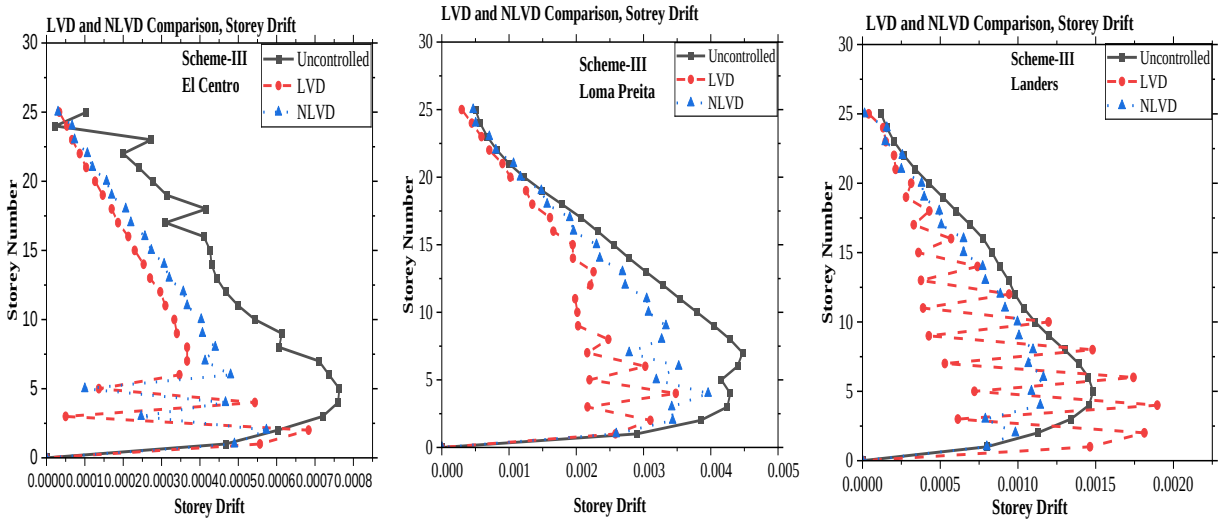


**Fig. 26 Comparison of LVD and NLVD storey drift with damper arrangement scheme-I and III under El Centro, Loma Preita and Landers earthquakes**

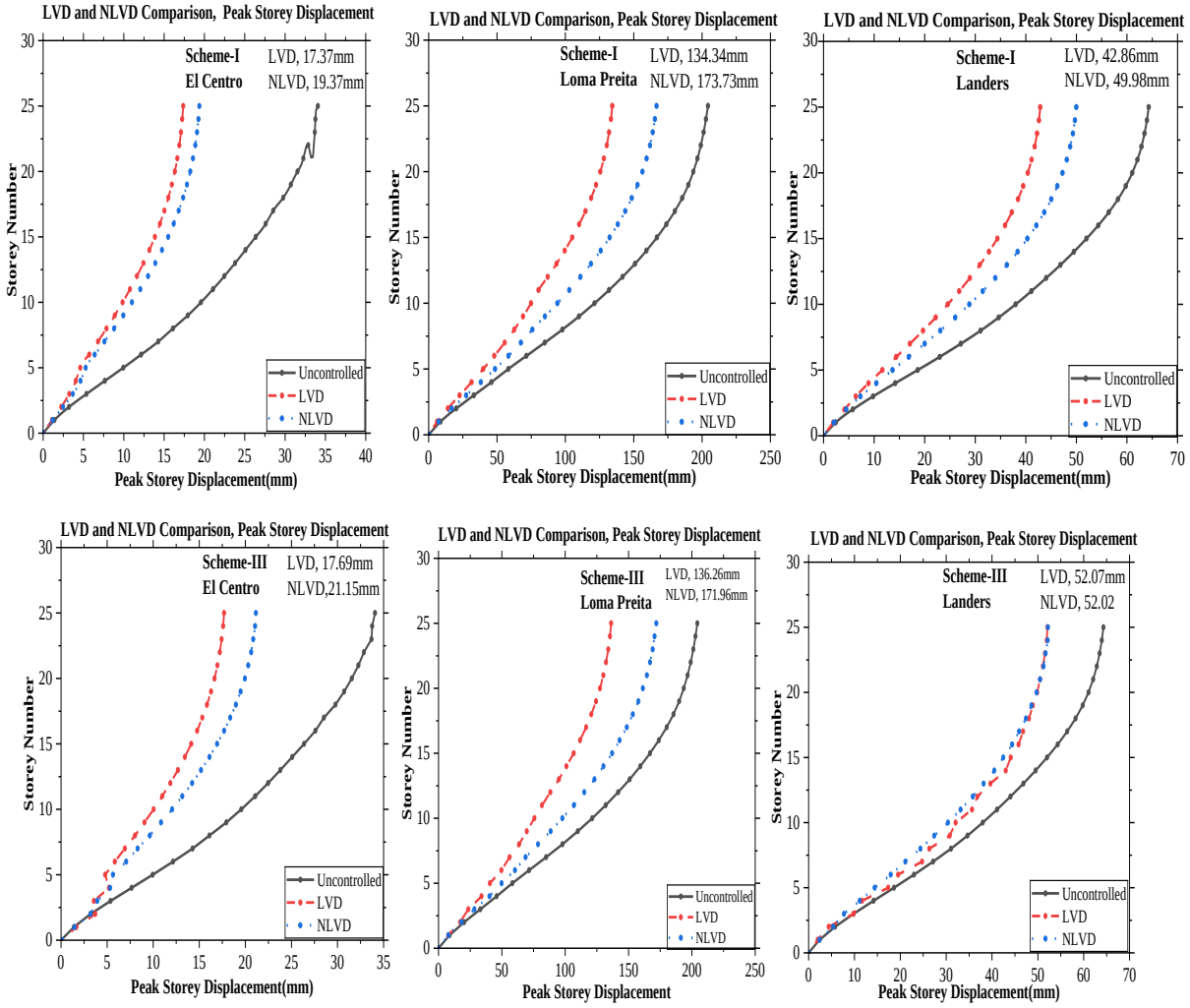


**Fig. 27 Comparison of LVD and NLVD damper with arrangement scheme-I and III, storey displacement under El Centro, Loma Preita and Landers earthquake**

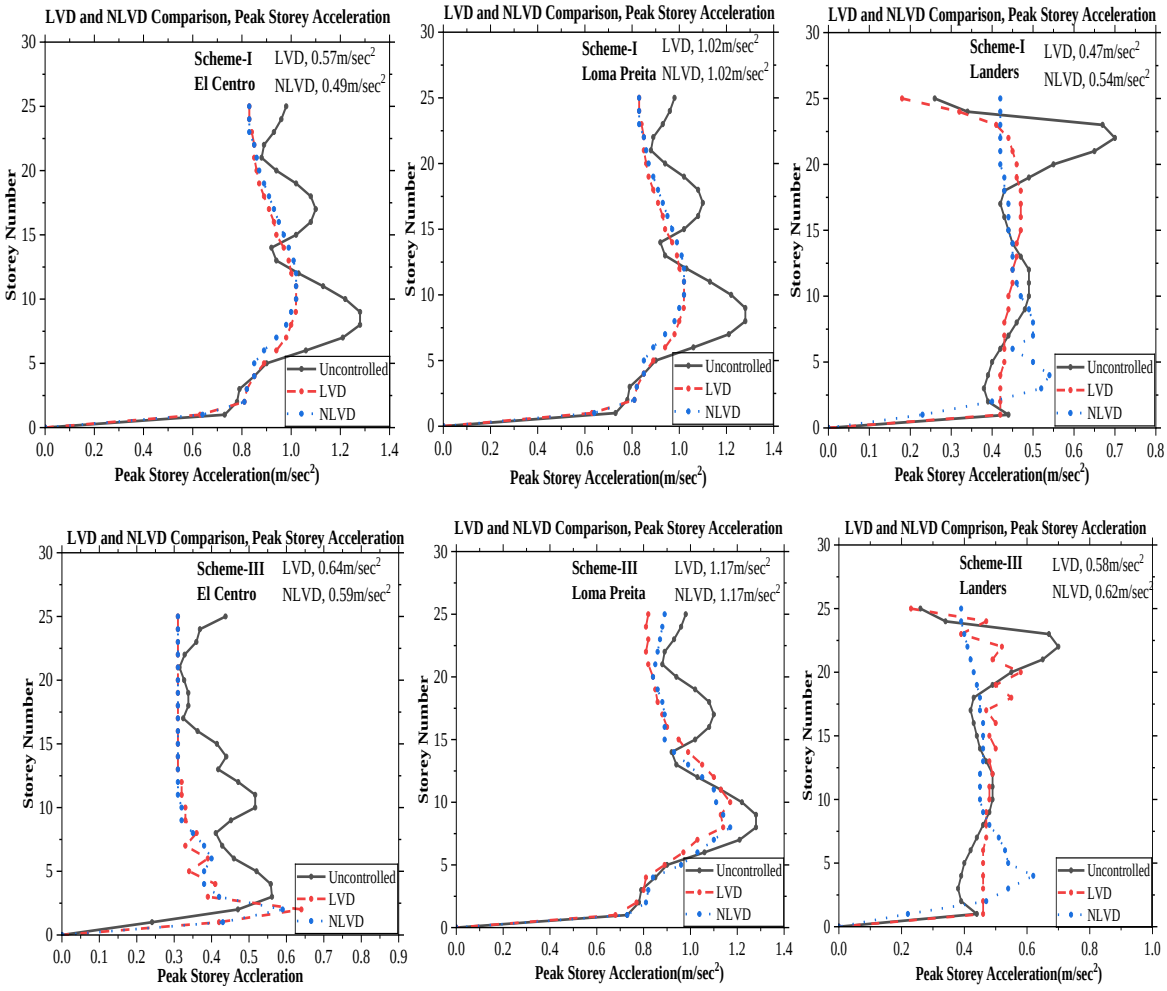


**Fig. 28 Comparison of LVD and NLVD damper with arrangement scheme-I and III, storey peak acceleration under El Centro, Loma Preita and Landers earthquake**

From Figure 28, the storey acceleration is more between storey 5 to 10. Storey peak response reduces by 33% with scheme-I and 17% with scheme III. LVD reduces slightly more, with 5% to 7% peak acceleration than NLVD.

## 7. Conclusion

A numerical study of a seismically excited 25-storey tall reinforced cement concrete building is carried out under six real ground motions. The building is symmetric. The uncontrolled response of tall buildings is compared with software ETABS and MATLAB programs. The 25-storey tall building is installed with the devices installed with earlier mentioned scheme-I and innovative scheme-II and III. The responses are evaluated for two types of dampers, linear viscous damper and nonlinear viscous damper, using the aforementioned damper location schemes. The damping coefficient is varied for LVD and NLVD with considered velocity exponent α, looking at the overall performance of dampers. The controllability index is determined, and damping coefficients for LVD and NLVD are optimized. The response of tall buildings under six ground motions with separately installed LVD and NLVD with the above-mentioned damper installation schemes are investigated, and a comparative study for LVD and NLVD is carried out to determine the best suitable damper location scheme for both types of passive dampers. Based on the trends observed in the numerical results of the present study, the following conclusions can be drawn:

1. The damping coefficient of the passive damper is significantly lower for the tall building equipped with a nonlinear viscous damper compared to a linear viscous damper, making it a more economical damper design.
2. The LVD installed with damper arrangement scheme-I reduces the peak displacement responses of tall buildings by 34% to 50%, depending on the characteristics of considered ground motion. The NLVD with the same installation scheme reduces displacement response from 28% to 43%. The numerical differences between these responses are 5% to 10%; hence, NLVD with damper with damper arrangement scheme-I proves to be better than LVD.

3. The LVD, with damper installation scheme-II, reduces the peak displacement response of tall buildings by 17% to 33%. The NLVD with scheme- II reduces the displacement responses by 11% to 24%, which indicates that the damper arrangement scheme-I is comparatively suitable against the scheme-IIs.
4. The LVD installed with damper arrangement scheme-III, top storey peak displacement is reduced by about 48%, and for the same damper arrangement scheme with NLVD, it is by 38%; hence, the damper arrangement scheme-III is quite effective in response control compared to scheme-II.
5. The reduction in peak displacement response for the tall building installed with LVD and NLVD with damper arrangement scheme-I and Scheme-III are almost similar; hence, it can be concluded that the damper arrangement scheme-III is superior out of all damper arrangement schemes, which requires less than half numbers of dampers shows economic advantages.
6. The acceleration response is reduced for the tall building installed with LVD with installation schemes I, II, and III by 45% to 55%, and for the same installation schemes with NLVD, it is 40% to 55%. It means that, with the same damper installation scheme, the peak acceleration response reduction difference is quite small.
7. The storey drift, storey displacement and storey acceleration responses are reduced considerably with installation scheme-I compared and scheme-III as compared to scheme-II. Also, LVD reduces the above response slightly more compared to NLVD.
8. Larger damper forces are generated by all NLVD dampers under various earthquakes and arrangement schemes compared to LVD, dissipating a huge amount of seismic energy.
9. The above parameters are evaluated, and with the acceptable 5-10% response variation for the tall building installed with LVD and NLVD, it can be said that a lesser value of damping coefficient is required for NLVD compared to LVD, making NLVD superior and economical.
10. Controllability index, $R_e$ depends on the value of the damping coefficient (C).

## References


[1] M.D. Symans, and M.C. Constantinuo, "Passive Fluid Viscous Damping Systems for Seismic Energy Dissipation," *ISET Journal of Earthquake Technology*, vol. 35, no. 4, pp. 185-206, 1998. [Google Scholar] [Publisher Link]

[2] M.D. Symans et al., "Semi Active Fluid Viscous Dampers for Seismic Response Control," *First World Conference on Structural Control*, pp. 1-12, 1994. [Google Scholar] [Publisher Link]

[3] Rakesh K. Goel, "Effect of Supplemental Viscous Damping on Seismic Response of Asymmetric-Plan System," *Earthquake Engineering and Structural Dynamics*, vol. 27, no. 2, pp. 125-141, 1998. [CrossRef] [Google Scholar] [Publisher Link]

[4] T.T. Soong, and G.F. Dargus, *Passive Energy Dissipation and Active Control*, Structural Engineering Handbook, CRC Press, 2002. [Google Scholar] [Publisher Link]

[5] D. Lee, and D.P. Taylor, "Viscous Damper Development and Future Trends," *The Structural Design of Tall Buildings*, vol. 10, no. 5, pp. 311-320, 2001. [CrossRef] [Google Scholar] [Publisher Link]

[6] Robert J. McNamara, and Douglas P. Taylor, "Fluid Viscous Dampers for High Rise Buildings," *The Structural Design Tall and Special Buildings*, vol. 12, no. 2, pp. 145–154, 2003. [CrossRef] [Google Scholar] [Publisher Link]

[7] Henry C. Huang, "Efficiency of the Motion Amplification Device with Viscous Dampers and Its Application in High Rise Buildings," *Earthquake Engineering and Engineering Vibration*, vol. 8, pp. 521-536, 2009. [CrossRef] [Google Scholar] [Publisher Link]

[8] Matt Jackson, and David M. Scott, "Increasing Efficiency of Tall Building by Damping," *ASCE Structures Congress*, pp. 3132-3142, 2010. [CrossRef] [Google Scholar] [Publisher Link]

[9] M. Sarkisiana et al., "Achieving Enhanced Seismic Design Using Viscous Damping Technology," *Structures Congress 2013: Bridging Your Passion with Your Profession*, pp. 2729-2744, 2013. [CrossRef] [Google Scholar] [Publisher Link]

[10] Ding Kun et al., "Application of Viscous Dampers for Super Tall Residential Buildings in High-Wind Strong-Seismic Area," *Proceedings of the 2016 World Congress on Advances in Civil, Environmental, and Materials Research (ACEM16)*, 2016. [Google Scholar] [Publisher Link]

[11] Jianbing Chen, Xiaoshu Zeng, and Yongbo Peng, "Probabilistic Analysis of Wind-Induced Vibration Mitigation of Structures by Fluid Viscous Dampers," *Journal of Sound and Vibration*, vol. 409, pp. 287-305, 2017. [CrossRef] [Google Scholar] [Publisher Link]

[12] Tathagata Roy, and Vasant Matsagar, "Effectiveness of Passive Response Control Devices in the Building under Earthquake and Wind During Designing Life," *Structure and Infrastructure Engineering*, vol. 15, no. 2, pp. 252-268, 2018. [CrossRef] [Google Scholar] [Publisher Link]

[13] B.G. Kavyashree, Shantharam Patil, and Vidya S. Rao, "Review on Vibration Control in Tall Buildings: From Perspective of Devices and Applications," *International Journal of Dynamics and Control*, vol. 9, pp. 1316-1331, 2021. [CrossRef] [Google Scholar] [Publisher Link]

[14] A. Shariati, R. Kamgar, and R. Rahgozar, "Optimum Layout of Nonlinear Fluid Viscous Damper for Improvement the Responses of Tall Buildings," *International Journal of Optimization in Civil Engineering*, vol. 10, no. 3, pp. 411-413, 2020. [Google Scholar] [Publisher Link]

[15] Miguel Martinez-Paneda, and Ahmed. Y. Elghazouli, "Optimal Application of Fluid Viscous Dampers in Tall Buildings Incorporating Integrated Damping System," *The Structural Design of Tall and Special Buildings*, vol. 30, no. 17, 2021. [CrossRef] [Google Scholar] [Publisher Link]

[16] Xiameng Huang, and Jaehoon Bae, "Evaluation of Genetic Algorithms for Optimizing the Height Wise Viscous Damper Distribution in Regular and Irregular Buildings," *Arabian Journal of Science and Engineering*, vol. 47, pp. 1245-12962, 2022. [CrossRef] [Google Scholar] [Publisher Link]

[17] Gary C. Hart, and Kevin Wong, *Structural Dynamics for Structural Engineers*, John Wiley & Sons, 2000. [Google Scholar] [Publisher Link]

[18] Alberto Lago, Dario Trubucco, and Antony Wood, *Damping Technologies for Tall Buildings, Theory, Design Guidance and Case Studies*, Elsevier Science, pp. 1-1124, 2018. [Google Scholar] [Publisher Link]

[19] *Quantification of Building Seismic Performance Factor*, U.S. Department of Homeland Security, FEMA, 2009. [Google Scholar] [Publisher Link]